

SPRINGER BRIEFS IN
APPLIED SCIENCES AND TECHNOLOGY

Mahesh Patil
Pankaj Rodey

Control Systems for Power Electronics A Practical Guide

 Springer

**SpringerBriefs in Applied Sciences
and Technology**

More information about this series at <http://www.springer.com/series/8884>

Mahesh Patil · Pankaj Rodey

Control Systems for Power Electronics

A Practical Guide

 Springer

Mahesh Patil
Secunderabad
India

Pankaj Rodey
Embedded Control Systems
Hyderabad
India

ISSN 2191-530X ISSN 2191-5318 (electronic)
SpringerBriefs in Applied Sciences and Technology
ISBN 978-81-322-2327-6 ISBN 978-81-322-2328-3 (eBook)
DOI 10.1007/978-81-322-2328-3

Library of Congress Control Number: 2015934946

Springer New Delhi Heidelberg New York Dordrecht London

© The Author(s) 2015

This work is subject to copyright. All rights are reserved by the Publisher, whether the whole or part of the material is concerned, specifically the rights of translation, reprinting, reuse of illustrations, recitation, broadcasting, reproduction on microfilms or in any other physical way, and transmission or information storage and retrieval, electronic adaptation, computer software, or by similar or dissimilar methodology now known or hereafter developed.

The use of general descriptive names, registered names, trademarks, service marks, etc. in this publication does not imply, even in the absence of a specific statement, that such names are exempt from the relevant protective laws and regulations and therefore free for general use.

The publisher, the authors and the editors are safe to assume that the advice and information in this book are believed to be true and accurate at the date of publication. Neither the publisher nor the authors or the editors give a warranty, express or implied, with respect to the material contained herein or for any errors or omissions that may have been made.

MATLAB[®] and Simulink[®] are registered trademarks of The MathWorks, Inc. All other trademarks are the property of their respective owners. For MATLAB and Simulink product information, please contact: The MathWorks, Inc. 3 Apple Hill Drive Natick, MA, 01760-2098 USA, Tel: 508-647-7000, Fax: 508-647-7001, E-mail: info@mathworks.com, Web: <http://www.mathworks.com>

Printed on acid-free paper

Springer (India) Pvt. Ltd. is part of Springer Science+Business Media (www.springer.com)

Foreword

It has been a few years since I have been working with the authors of this book on the field of control systems and power electronics. We have executed challenging programs together and during our conversations we often touched upon a requirement for a practical text on this subject. It gives me immense pleasure to write the foreword for this book and seeing a thought converted into productive action.

This book is different from existing books on *Control Systems for Power Electronics* in a way that it is not scholarly, but is a practical-oriented compilation, replete with simple industry case studies. The illustrations are lucid and supported with simulations for various conditions and topologies adding a lot of value for the reader. The simulations and the accompanying colored illustrations make the complicated concepts easy to understand giving the reader a comprehensive understanding of the subject. The visual insights are extremely helpful and do not make it necessary for the reader to be extensively engaged on mathematics of control theory. I recommend this book for all readers in this domain across research, academics, and industry.

I enjoyed this book and hope you enjoy it too!

Anusheel Nahar, CEO
Controltrix Corp

Preface

The scope of the book covers most of the aspects as a primer on power electronics starting from a simple diode bridge to a DC–DC convertor using PWM control. The thyristor-bridge and the mechanism of forming a closed-loop system are discussed in Chaps. 1–3. The concepts are applied in Chap. 4 as a case study for buck converter which uses MOSFETs as switching devices and the closed-loop system is elaborated in Chap. 5. Chapter 6 is focused on the embedded system basics and the implementation of controls in the digital domain. The reader will find it easy to work on the practical control systems with microcontroller implementation.

The primary intent of this book is to help the reader gain an accelerated learning path to practical control system engineering and transform control theory to an implementable control system through electronics. Illustrations are provided for most of the examples with fundamental mathematics along with simulations of the systems with their relevant equations and stability calculations.

There are books elaborating on power electronics devices, power electronics applications, microcontrollers, and control system theory which can be used as a reference by the reader. The difference between specialized books and this book is that this book focuses on building practical blocks leveraging a basic understanding of electronic devices, simulations, and microcontrollers.

After reading this book, engineers will have a sound understanding of practical control system engineering. This will help them apply their domain knowledge to real product development.

Acknowledgments

This book is an on the job approach to implementing control system theory to a practical control system for various applications. It has been an arduous effort to translate our learning to development of practical control systems in the analog and digital world and the prime motive of this book is the thought that some of the learnings can be consolidated to give a head start to a practicing engineer.

We have learned much through our experience in various organizations over the years, working with brilliant colleagues and facing technical challenges in our everyday work.

Our sincere thanks to our colleagues at Crompton Greaves, General Electric, Emerson with whom our decades of association enlightened us on various aspects of this subject. Our special thanks to Shijin Krishna, who meticulously worked on the equations and helped through the proofreading with all his patience.

Our special thanks to Somachand Kattige and Rathish Gangadharan, who spent their precious time reviewing the text and suggesting improvements.

To our family and friends who had enormous patience to stand by us during this period of writing during weekends and late nights and encouraging us to go the last mile in making the book as flawless as possible.

Contents

| | | |
|----------|--|----|
| 1 | Uncontrolled Rectifier | 1 |
| | Rectifier Configurations | 1 |
| 2 | Controlled Rectifier | 9 |
| | Introduction | 9 |
| | The Thyristor Rectifier | 10 |
| 3 | Thyristor Rectifier in Closed Loop | 15 |
| | An Introduction to Closed-Loop Control | 15 |
| | Power Circuit Explanation | 16 |
| 4 | Buck Converter in Open Loop | 21 |
| | An Introduction to Open Loop | 21 |
| | Mathematical Modeling of the Power Converter | 24 |
| | The Control of the Buck Converter | 25 |
| | Voltage Mode Control of Buck Converter | 26 |
| 5 | Buck Converter in Closed Loop | 29 |
| | An Introduction to Closed Loop | 29 |
| 6 | Design of Embedded Control | 39 |
| | Introduction | 39 |
| | Analog and Digital Control | 39 |
| | Developing an Embedded Controller | 41 |
| | A Brief Introduction to Model-Based Design | 44 |

- 7 Case Study of an Embedded Control System Design 45**
- Introduction 45
- Application Overview. 46
- Measurement of Speed of the Motor 46
 - Hall Effect Sensor 46
 - Opto Coupler 47
 - Controlling the Speed with PWM 48
- Subsystem Design 48
- PCB Layout for the System 50
- Conclusion 51

- References. 53**

Figures

| | | |
|----------|---|----|
| Fig. 1.1 | Three-phase bridge rectifier | 2 |
| Fig. 1.2 | Phase voltages for three-phase bridge rectifier | 4 |
| Fig. 1.3 | Line to line voltages for three-phase bridge rectifier | 4 |
| Fig. 1.4 | Diode bridge with resistive load ($R = 100 \Omega$, $L = 0$ H) | 5 |
| Fig. 1.5 | Diode bridge with resistive inductive load ($R = 100 \Omega$, $L = 0.1$ H). | 5 |
| Fig. 1.6 | Diode bridge with resistive inductive load ($R = 100 \Omega$, $L = 1$ H) | 6 |
| Fig. 2.1 | Power scheme in a typical industrial application | 10 |
| Fig. 2.2 | Three-phase thyristor bridge | 10 |
| Fig. 2.3 | The waveform for input voltage firing sequence, output voltage and output current for $R = 100 \Omega$, $L = 0$ H, firing angle of 45° | 12 |
| Fig. 2.4 | The waveform for input voltage firing sequence, output voltage and output current for $R = 100 \Omega$, $L = 0.1$ H, firing angle of 45° | 12 |
| Fig. 2.5 | The waveform for input voltage firing sequence, output voltage and output current for $R = 100 \Omega$, $L = 1$ H, firing angle of 45° | 13 |
| Fig. 3.1 | Block diagram representation of a closed-loop control system | 16 |
| Fig. 3.2 | Three-phase thyristor rectifier in closed loop | 17 |
| Fig. 3.3 | VDC and LDC waveform for $P-I$ gains ($P = 100$, $I = 0$). | 17 |
| Fig. 3.4 | VDC and LDC waveform for $P-I$ gains ($P = 100$, $I = 50$). | 18 |
| Fig. 4.1 | The buck converter circuit. The <i>arrow</i> represents the power switch which is switched ON and OFF at very high frequency. The direction of the <i>arrow</i> is the direction of flow of current when the switch is turned ON | 22 |
| Fig. 4.2 | The buck converter circuit when the switch is switched ON. | 22 |
| Fig. 4.3 | The buck converter circuit when the switch is switched OFF | 23 |
| Fig. 4.4 | Mathematical model of the open-loop buck converter | 26 |
| Fig. 5.1 | The buck converter in voltage mode control. | 30 |

Fig. 5.2 The buck converter in voltage mode control. For $P = 0.05$, $I = 0$, $D = 0$, the ‘Error’ between the reference (80 V) and actual voltage is ~ 72 V, thus the output voltage is 8 V, far off from the desired 80 V reference 31

Fig. 5.3 Output DC voltage of the buck converter. A large ripple is seen in the output voltage for a significantly large P gain of $K_p = 100$, $K_i = 0$, $K_d = 0$ 31

Fig. 5.4 The buck converter in voltage mode control for $K_p = 10$, $K_i = 0$, $K_d = 0$ 32

Fig. 5.5 Simulink oscilloscope for output voltage. For $K_p = 100$, $K_i = 0$, $K_d = 0$, there is a steady-state error of 4 V in the output voltage of the converter 33

Fig. 5.6 The buck converter in voltage mode control for $K_p = 10$, $K_i = 3$, $K_d = 0$ 33

Fig. 5.7 Simulink[®] oscilloscope for output voltage. For $K_p = 100$, $K_i = 3$, $K_d = 0$, the steady-state error in the output voltage progressively decreases and becomes zero after ~ 9 s 34

Fig. 5.8 Output voltage of the converter. Plot of the output voltage of the converter in the conditions, same as in Fig. 5.4. The transience in the system is more pronounced at start-up, as shown in the *marked section* in the plot 35

Fig. 5.9 Plot of the output voltage of the converter with the initial 25 ms zoomed 35

Fig. 5.10 The buck converter in voltage mode control for $K_p = 10$, $K_i = 3$, $K_d = 0.0001$ 36

Fig. 5.11 Plot of the output voltage of the converter with $K_p = 10$, $K_i = 3$, $K_d = 0.0001$. Due to the integrating effect of the I controller, the steady-state error progressively decreases and also the initial transient response is improved, as shown in the next plot. 36

Fig. 5.12 Plot of the output voltage of the converter initial 20 ms zoomed. It is evident that the voltage stabilizes faster, in about 14 ms, compared to ~ 25 ms as shown in Fig. 5.8, without the D controller. 37

Fig. 6.1 Buck converter block diagram with analog controller 40

Fig. 6.2 Buck converter block diagram with digital controller. 41

Fig. 6.3 First-order low pass filter. 42

Fig. 7.1 Speed control of DC motor using PWM technique with Hall effect sensor 46

Fig. 7.2 Hall effect sensor 47

Fig. 7.3 Opto coupler MCT2E 47

Fig. 7.4 Opto coupler details 48

Fig. 7.5 Pin out of ATtiny2313 49

Fig. 7.6 System schematic 50

Fig. 7.7 PCB layout 51

Learn from the Experts

This book is intended for beginners in control systems and also for professional engineers who work on controlling machines using the blend of power electronics and embedded control. Having gone through the learning curve and not found any concise material we decided to put together our limited learnings for our own reference and also for the larger forums.

The primary intent of this material is to get expertise in practical control system engineering with a motive of transforming control theory to an implementable control system in a microcontroller and electronics.

About the Authors



nals. He holds a Master's qualification from XLRI.

Mahesh Patil is a technopreneur and has led teams focusing on cutting edge technologies working for Multinational companies like General Electric, Crompton Greaves and has his own startup. He has built high performing start-up teams for electric vehicles, embedded services, expertise in building strategic alliances with high-tech companies. His experiences include product development for Industrial, Energy, and Automotive sectors working for large MNCs and also his own start-up organization. He is six sigma certified and has published papers in various international jour-



Pankaj Rodey is a technical specialist in Embedded Control Systems domain. He has vast experience in the field of control systems for power generation and power electronics. He is an expert in model-based virtual prototyping and design of embedded controls for power electronics and power generation products. He holds six sigma certificates and a Bachelor's degree in Electrical Engineering from NIT Nagpur.

Chapter 1

Uncontrolled Rectifier

Abstract This chapter discusses the basic power electronics switch and the various configurations of the diode bridge forming the foundation for the control systems application for power electronics. The resulting waveforms and the equations are elaborated which will form the basis for a detailed understanding of controllable power devices and implementation of control strategies.

Keywords Diode · Thyristor · MOSFET · IGBT · Rectifier · Commutation · Resistance · Inductance

The diode forms the first semiconductor device we come across in academics and applied in product development life cycles and is the fundamental two terminal semiconductor switch, ubiquitous in electronics applications. Though the diode is a simple two-terminal device, a detailed understanding of the diode rectifier application is a prerequisite for understanding more complex semiconductor switches like Thyristors, MOSFETS, and IGBTs. A majority of our everyday applications like the power supplies in our computers, home appliances, and automobile electronics have these devices.

A rectifier is classified based on the configuration of these diodes in an electronic circuit and the classification depends on the number of diodes. The term rectifier is referred to the operation of converting an AC voltage to a DC voltage or an AC current to a DC current.

We will explore the most commonly used rectifier configurations.

Rectifier Configurations

We will work on the three-phase diode bridge as our first application. The key attributes to study in a three-phase bridge rectifier are instants at which the diode turns ON and turns OFF. The impact of the load on the rectifier, which can be a purely resistive load, an inductive load, or a combination of both, will be studied. The source resistance and inductance also form a very important parameter for the

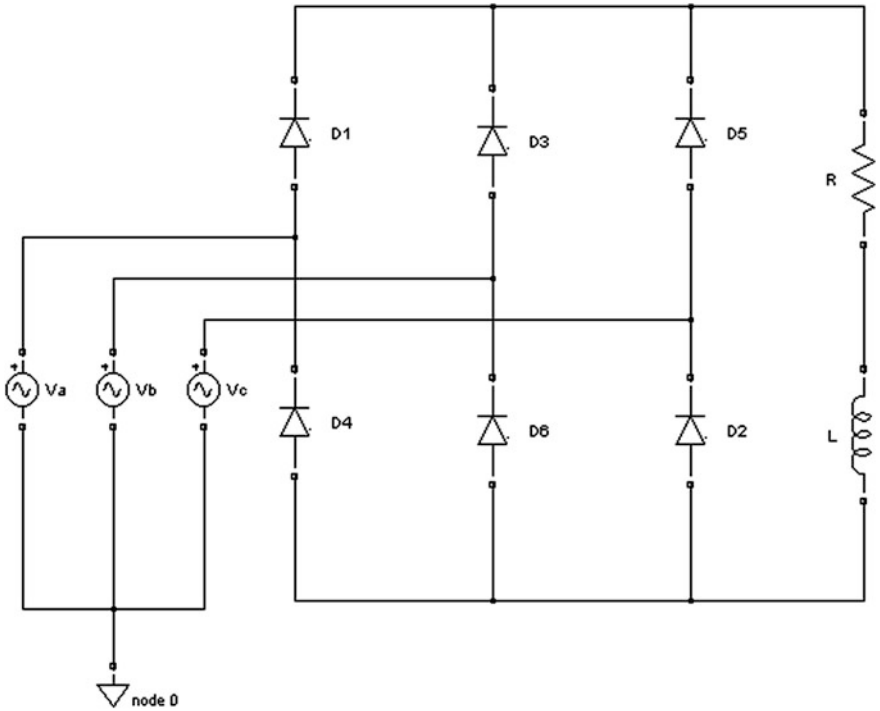


Fig. 1.1 Three-phase bridge rectifier

behavior of the bridge. The nature of the load on the bridge rectifier governs the profile of the output current of the rectifier, ripple on the dc voltage, and current.

Figure 1.1 gives the detailed circuit diagram of a three-phase bridge rectifier using diodes.

Figure 1.1 shows a three-phase diode bridge rectifier. The input to the rectifier is a balanced three phase.

AC voltage source denoted by V_a , V_b , V_c .

For simplification we assume the source impedance to be zero and the diodes as ideal switches. The load on the rectifier is a combination of resistive load and inductive load.

We will explore the behavior of the circuit for

1. Resistive load
2. Resistive-Inductive load

The current waveforms and the voltage waveforms for various values of R and L will be studied. To begin with the values are taken as $R = 100 \Omega$ and $L = 0.1 \text{ H}$.

Table 1.1 shows the sequence of commutation of the diode bridge. The first column is the Line to Line voltages of the conduction legs of the bridge and the corresponding devices which are conducting on the legs. As is evident from the

Table 1.1 Sequence of conduction of diodes for the three-phase diode rectifier

| $L-L$ | Devices | |
|----------|---------|------------------|
| V_{ab} | 1, 6 | Top device ON |
| V_{ca} | 1, 2 | Bottom device ON |
| V_{bc} | 2, 3 | Top device ON |
| V_{ba} | 3, 4 | Bottom device ON |
| V_{ac} | 5, 4 | Top device ON |
| V_{cb} | 5, 6 | Bottom device ON |

table and the attached waveforms, the positive excursions of voltages mentioned in column 1 of the table forward bias the TOP devices. For example, the V_{ab} positive excursion at zero crossing forward biases Diode D1 and the negative excursion for the same forward biases Diode D4 ON. Behavior of the other diodes can be explained on the same lines based on line voltages of V_{bc} and V_{ca} .

The inductance on load governs the *time constant* of the system.

This switching pattern as explained and depicted in the waveforms forms the basis of understanding the diode bridge commutation.

The input three-phase voltage of the diode rectifier is represented mathematically as:

$$V_a = V_m * \sin(\omega t), \quad (1.1)$$

$$V_b = V_m * \sin(\omega t - 120), \quad (1.2)$$

$$V_c = V_m * \sin(\omega t + 120) \quad (1.3)$$

where V_m is the peak voltage from the utility supply. The line to line voltages are represented as:

$$V_{ab} = V_a - V_b, \quad V_{bc} = V_b - V_c, \quad V_{ca} = V_c - V_a \quad (1.4)$$

We will now see how the three-phase AC voltage is converted to DC by this *six pulse* rectifier. For simplification, consider a peak voltage V_m of 1 V. The plot of the phase voltages V_{an} , V_{bn} , V_{cn} is shown in Fig. 1.2.

A plot of the line to line voltages for the source is shown in Fig. 1.3

From this figure of phase to neutral voltages of the input, it is evident that during the interval of 30° – 150° , the phase to neutral voltage of phase a that is V_{an} is greater in value than phase to neutral voltages, V_{bn} and V_{cn} . So, during this interval, diode D1 will be forward biased.

Looking closely at the 20° time instant, V_{ab} is approximately 1.25 V and increasing in magnitude, V_{ca} is approaching 0 V and moving towards negative, V_{bc} is reducing in magnitude from -1.6 V to -1.5 V. Now, looking at the line to line voltages, it can be seen that during the interval of 30° – 90° , voltage V_{ab} is greater than the other line voltages V_{bc} and V_{ca} . So, during this interval, both diodes D1 and D6 will be forward biased and produce the rectified pulse across the load.



Fig. 1.2 Phase voltages for three-phase bridge rectifier

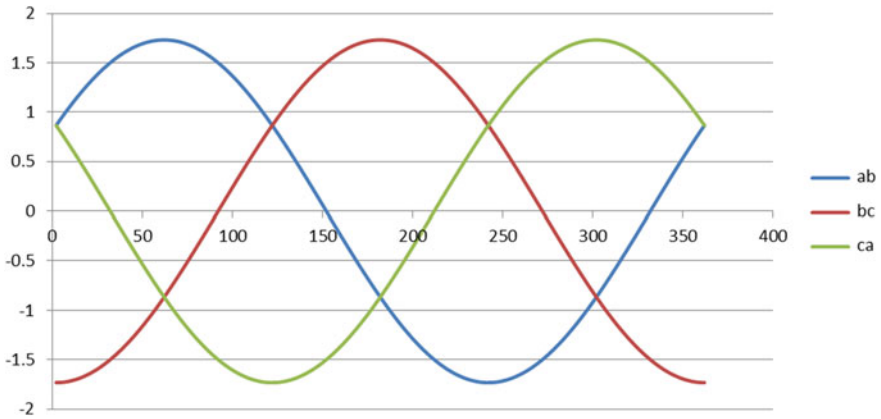


Fig. 1.3 Line to line voltages for three-phase bridge rectifier

From the waveforms of line to line voltages, it can be seen that during the interval of 90° – 150° , line voltage V_{ca} is at a negative extreme. This means $(V_a - V_c)$ is greater than the other line voltages V_{ab} and V_{bc} . So, during this interval both diodes D1 and D2 will be forward biased and produce the rectified pulse across the load.

As seen above, for the interval 30° – 150° , two rectified pulses will be produced across the load by pair D1, D6, and pair D1, D2. This is shown by the first two rows in Table 1.1.

On similar lines, from the table it can be seen how each pair of diodes produces a rectified pulse across the load.

Thus, for each 360° cycle of the line to line voltage, six rectified pulses are produced across the load and hence the name ‘*six pulse rectifier*’.

This is also shown in Figs. 1.4, 1.5 and 1.6, where the rectangular pulse at the bottom represents the instant at which the indicated pair of diodes starts to conduct.

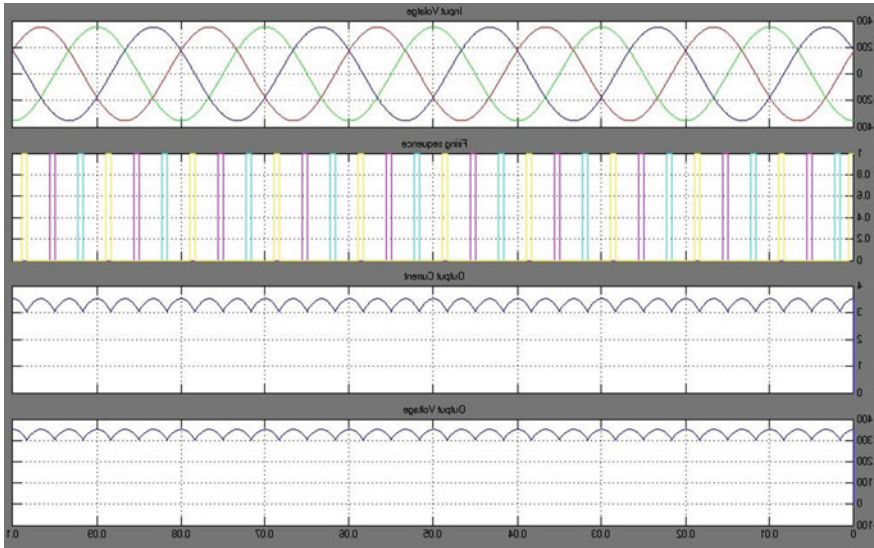


Fig. 1.4 Diode bridge with resistive load ($R = 100 \Omega$, $L = 0 \text{ H}$)

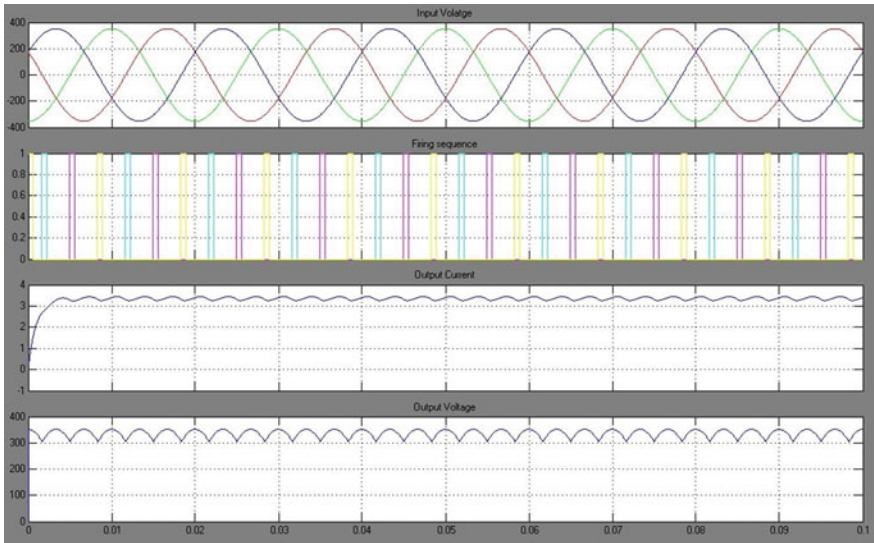


Fig. 1.5 Diode bridge with resistive inductive load ($R = 100 \Omega$, $L = 0.1 \text{ H}$)

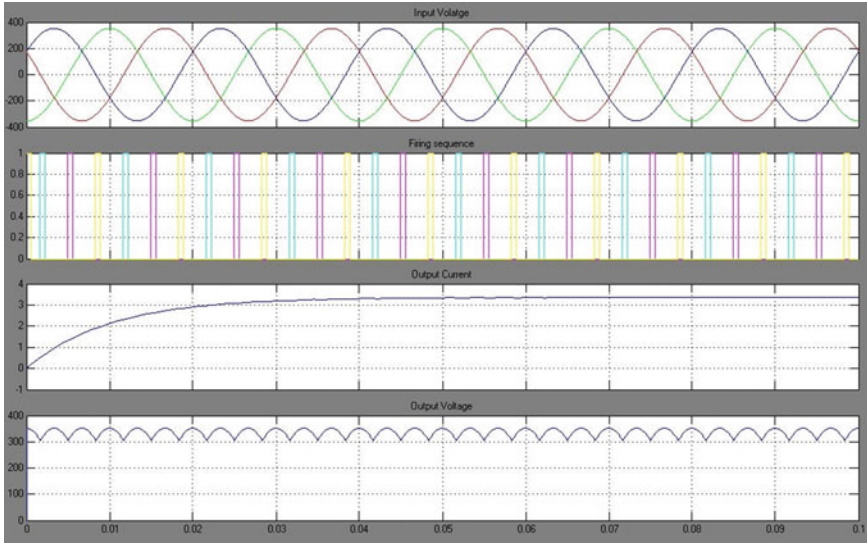


Fig. 1.6 Diode bridge with resistive inductive load ($R = 100 \Omega$, $L = 1 \text{ H}$)

An inherent phenomenon in a power electronics system is the deviation of the output of the system from the desired value, alternating above and below the desired output. This undesired phenomenon is called ‘*ripple*’.

Next, we will observe the effect of the inductance on the current profile. For three different values of inductances the ripple in output current will be measured.

As noted in Table 1.2 and also seen from the waveforms, the increase in inductance causes a reduction in the ripple and a corresponding increase in the rise time. The time constant of the current is based on the ratio of inductance to resistance and is evident from the table.

The parameters of time constant, ripple, and the sequence of the conduction of the diode pairs form the basis for bridge *control* with thyristors which will be studied in the next chapter.

Figure 1.4 show the profile of output current when the inductance value is 0. The profile of the current follows the DC voltage and is **in phase** with the voltage.

Table 1.2 Variation of current ripple with inductance

| Inductance H | Current min | Current max | Ripple | Time constant (L/R) (μs) | Rise time |
|-----------------|----------------|----------------|--------|--|--------------|
| 0.01 | 3.1 | 3.52 | 0.42 | 100 | 0 |
| 0.1 | 3.25 | 3.34 | 0.09 | 10 | 0.004 |
| 1 | 3.35 | 3.35 | 0 | 1 | 0.04 |

In Fig. 1.4 the input three phase voltages are shown as:

Yellow: V_{ab}

Light Green: V_{bc}

Pink: V_{ca}

The 'Firing Sequence' waveform shows the instance at which a particular pair of diodes is forward biased.

Figure 1.5 shows the profile of output current when the inductance value is 0.1 H and the ripple in the current is reduced and the current lags the DC voltage.

Figure 1.6 shows that the current rise is further delayed when the inductance value is 1 H and the ripple in the current is almost zero forming a pure DC waveform.

The output voltage of the rectifier is expressed in terms of the input voltage as:

$$V_o = 3 * \sqrt{3} * \frac{V_m}{\pi} \quad (1.5)$$

where:

V_o Average voltage output from the converter

V_m Peak of the input voltage

The uncontrolled rectifier topologies with equations discussed in this chapter form the foundation for the controlled rectifier discussions in the next chapter.

Chapter 2

Controlled Rectifier

Abstract This chapter discussed the variants of thyristor based power electronics for different firing angles and the different combinations of the load like the resistance and the Inductance. The illustrations of the topologies with waveforms in Simulink[®] are demonstrated.

Keywords Firing angle · Ripple

Introduction

In the last chapter, we studied the uncontrolled bridge rectifier. The parameters for R and L were varied and the effect of this variation on output voltage and current of the rectifier was studied. In practical applications it is required to control the voltage and current at the DC link.

The block diagram (Fig. 2.1) represents a typical system in an industrial application. As discussed in the previous chapter, AC voltage source from a utility supply is rectified to DC using power electronics devices (diodes as explained chapter) and connected to a load that requires DC voltage and current. The utility generator generates a voltage that is not constant and varies in a certain range. According to Eq. (1.5) in the previous chapter, a change in AC voltage would cause a proportional change in the DC voltage.

A load in an industrial application is generally designed such that it requires a constant DC voltage and any change in DC voltage will cause undesired behavior of the load. Since the load and the AC utility are not controllable and the load requires a constant DC voltage, the only way to maintain the voltage for the load constant is to control the Power Electronics devices, such that the output from the circuit consisting of these devices can be controlled to a value required by the load. Such devices that can be controlled to maintain the voltage required by the load are called ‘*controlled devices*’. A **thyristor** forms the very basic of controlled device.

The Thyristor Rectifier

Figure 2.2 shows the three-phase Thyristor Bridge. The circuit is similar to the diode bridge described in Chap. 1, with the diodes replaced with Thyristors. A thyristor is a three-terminal device, somewhat similar to a junction transistor. When a small current flows into the Gate terminal, a current flow is established from anode to cathode. This is called the ON condition of the thyristor. When the AC voltage across the device is negative, the current from anode to cathode stops. This is called OFF condition of the thyristor. There are other techniques to have a better control on the instance at which the thyristor turns OFF. Such techniques are called ‘Commutation techniques’, which will not be discussed in this book.

In the 360° of the sine wave of the input AC voltage, the *Firing Angle* is the instance (in terms of degrees) when the device is turned ON. This instance is typically in the positive half of the AC voltage across the device. In most literatures, this angle is denoted by the Greek letter alpha and generally varies from 0° to 180° .

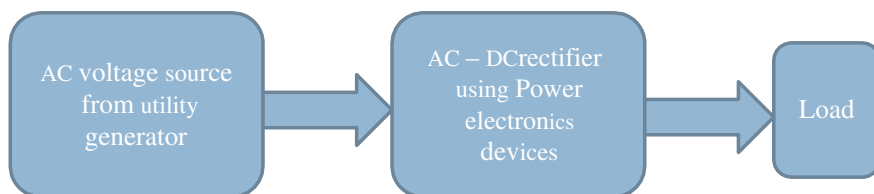


Fig. 2.1 Power scheme in a typical industrial application

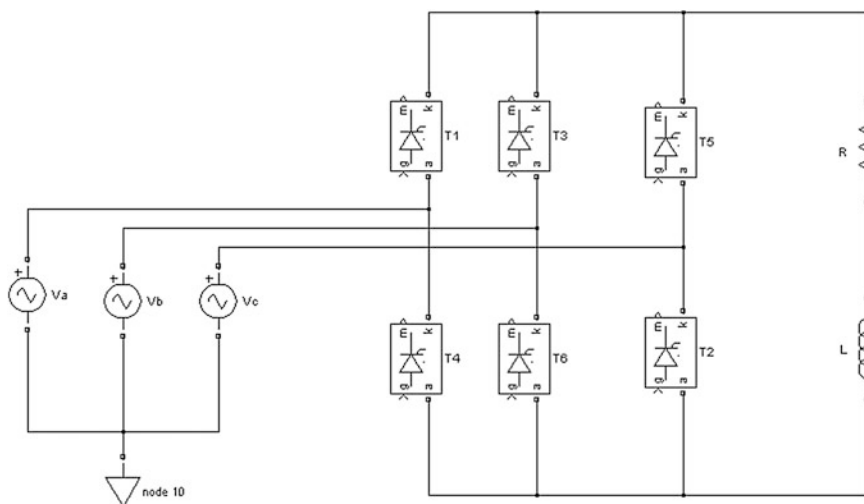


Fig. 2.2 Three-phase thyristor bridge

Table 2.1 Table for design of experiments for studying effect of firing angle on the operation of the thyristor rectifier. The Discontinuous term mentioned in the table indicates the DC link current I_{dc} is zero

| $VL-L$ | Firing angle degree | Cosine | V_{dc} | I_{dc} | Current ripple |
|-----------------------|---------------------|----------|----------|----------|----------------|
| Time constant = 0 | | | | | |
| 250 | 0 | 1 | 336 | 3.36 | 0.48 |
| 250 | 30 | 0.866158 | 296 | 2.96 | 2 |
| 250 | 45 | 0.707388 | 249 | 2.49 | 2.5 |
| 250 | 59 | 0.515485 | 194 | 1.95 | 3.01 |
| 250 | 60 | 0.50046 | 194 | 0 | Discontinuous |
| E | Firing degree | Cosine | V_{dc} | I_{dc} | Current ripple |
| Time constant = 0.001 | | | | | |
| 250 | 0 | 1 | 336 | 3.35 | 0.18 |
| 250 | 30 | 0.866158 | 296 | 2.915 | 0.7 |
| 250 | 45 | 0.707388 | 296 | 2.92 | 0.95 |
| 250 | 60 | 0.50046 | 190 | 1.7 | 1.15 |
| 250 | 75 | 0.25946 | 132 | 0.94 | 1.2 |
| 250 | 76 | 0.242574 | 0 | 0 | Discontinuous |
| E | Firing degree | Cosine | V_{dc} | I_{dc} | Current ripple |
| Time constant = 0.1 | | | | | |
| 250 | 45 | 0.707388 | 296 | 2.92 | 0 |

Figure 2.2 shows a three-phase thyristor bridge with an $R-L$ load.

Table 2.1 shows the details of a design of experiments performed with the circuit shown in Fig. 2.2 for a variation of Firing angle and the load. The variation of load is expressed in terms of the ratio L/R , shown as ‘Time Constant’.

As mentioned in Chap. 1, an inherent phenomenon in a power electronics system is the deviation of the output of the system alternating above and below the desired output. This undesired phenomenon is called ‘ripple’. The table also shows the effect of inductance and firing angle on the peak to peak ripple of the output current.

A model is shown in Fig. 2.2, created using MATLAB[®], and Simulink[®] and the parameters mentioned in this table are measured from the Simulink[®] model (Figs. 2.3, 2.4 and 2.5).

From Table 2.1, it can be seen that the DC voltage V_{dc} and the DC current I_{dc} change with the firing angle α . The magnitude of the DC link voltage and current reduces as the firing angle increases and the ripple in DC voltage and current increases due to the discontinuity in the current. As the inductance increases the ripple decreases due to the increased time constant.

Mathematically, for a three-phase thyristor converter, the output voltage is related to input voltage and the firing angle, expressed as:

$$V_o = 3 * \sqrt{3} * (V_m / \pi) * \cos \alpha \tag{2.1}$$

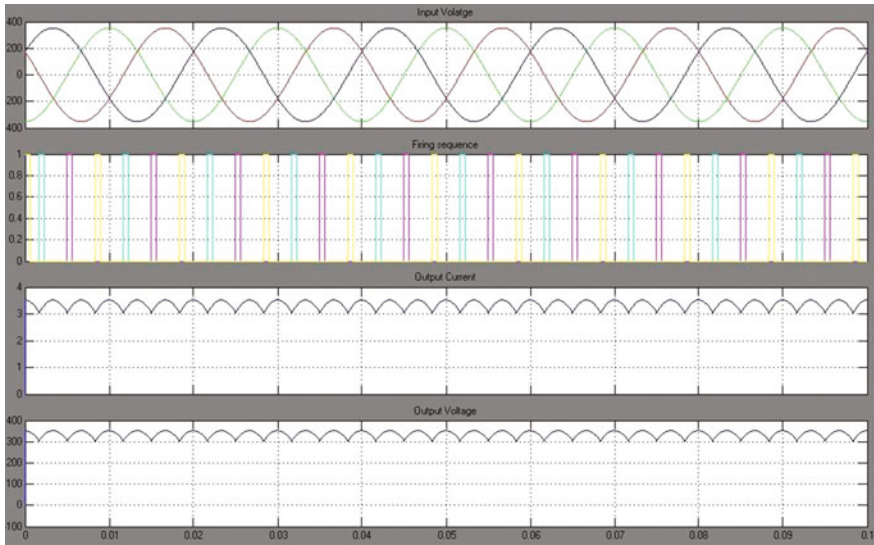


Fig. 2.3 The waveform for input voltage firing sequence, output voltage and output current for $R = 100 \Omega$, $L = 0 \text{ H}$, firing angle of 45°

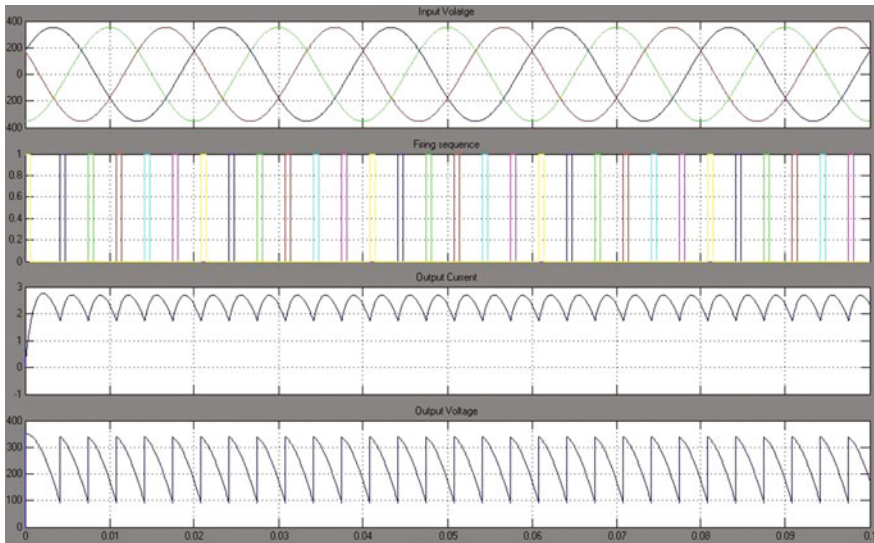


Fig. 2.4 The waveform for input voltage firing sequence, output voltage and output current for $R = 100 \Omega$, $L = 0.1 \text{ H}$, firing angle of 45°

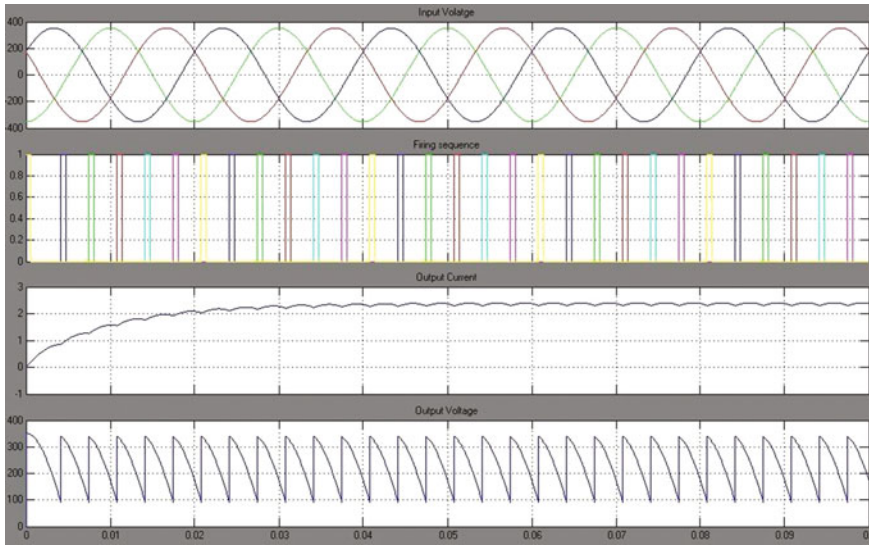


Fig. 2.5 The waveform for input voltage firing sequence, output voltage and output current for $R = 100 \Omega$, $L = 1 \text{ H}$, firing angle of 45°

where:

V_o Average voltage output from the converter

V_m Peak of the input voltage

α Firing angle

The observations in the DoE are also further detailed in terms of the waveforms of output voltage, output current, and the input voltage are shown in Figs. 2.3, 2.4 and 2.5.

Thus, the primary purpose of the inductance in the power circuit of the thyristor converter is to reduce the ripple in the output voltage and current.

A typical industrial Power Electronic system consists of two major parts, i.e., the *Power circuit* and the *Control circuit*. In this chapter the power circuit of the thyristor rectifier was explained with the DoE and instantaneous waveforms of the input and output.

The next chapter will deal with the basics of closed loop control and the Control circuits used in power electronics systems.

Chapter 3

Thyristor Rectifier in Closed Loop

Abstract This chapter discusses the closed-loop control system for a thyristor bridge. It has the step response demonstrated using a thyristor-based model and the corresponding waveforms are illustrated. This forms the basis for the next chapters on the elaborated control design using P , I , and D parameters.

Keywords Reference · Plant · Laplace · Controller · Feedback · Steady state · Integrator

An Introduction to Closed-Loop Control

The block diagram of Fig. 3.1 represents a control system in closed loop in terms of Laplace transform.

The figure shows a basic block diagram for a closed-loop control system. The purpose of a closed-loop control is to set the *Output* of the system equal to the *Reference* input. In the literature, the control system is represented as a block diagram with the terminology as follows:

Plant: The physical system, represented as a mathematical model. The Laplace transform is the standard transform used for representing the physical system.

Controller: This is the mechanism that *controls* the *control parameters* such that the output is equal to the reference input.

Feedback: The mechanism that differentiates the open-loop system from closed-loop control system. Feedback is the mechanism that connects the scaled output back to the input.

- $R(s)$: Reference input represented as a Laplace Transform. Ideally, the output should be equal to the reference at all instances
- $E(s)$: Error. This is the difference between the reference and feedback
- $G(s)$: Forward transfer function. This is the transfer function of the plant and the controller in cascade
- $H(s)$: Feedback path transfer function
- $C(s)$: The controller output, represented as a Laplace transform

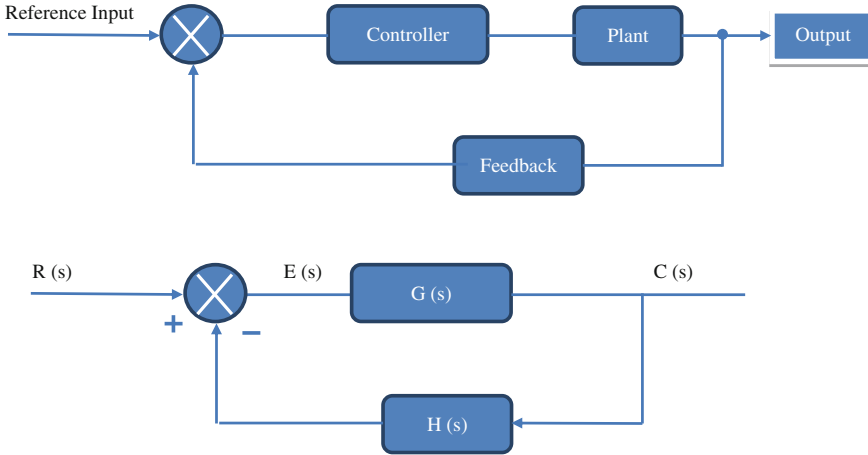


Fig. 3.1 Block diagram representation of a closed-loop control system

The blocks in the block diagram represent a mathematical *Gain*. Thus, the output of each block is the multiplication of the input to the block and the gain of the block. Thus, from the block diagram:

$$\begin{aligned}
 C(s) &= G(s) * E(s) \\
 C(s) &= G(s) * [R(s) - C(s) * H(s)] \\
 C(s) &= G(s) * R(s) - G(s) * C(s) * H(s) \\
 \frac{C(s)}{R(s)} &= \frac{G(s) * R(s)}{R(s)} - \frac{G(s) * C(s) * H(s)}{R(s)} \\
 \frac{C(s)}{R(s)} * [1 + G(s) * H(s)] &= G(s) \\
 \frac{C(s)}{R(s)} &= \frac{G(s)}{1 + G(s) * H(s)} \tag{3.1}
 \end{aligned}$$

This equation is called the ‘Closed-loop transfer function’ of the control system.

Power Circuit Explanation

Figure 3.2 shows a Simulink[®] model for six pulse Thyristor bridge converter with a three-phase input voltage. The three-phase input voltages are denoted by V_a , V_b , and V_c . The six pulse thyristor bridge is denoted by block ‘Thyristor Converter’. This block is the representation of six thyristors connected to the three-phase input

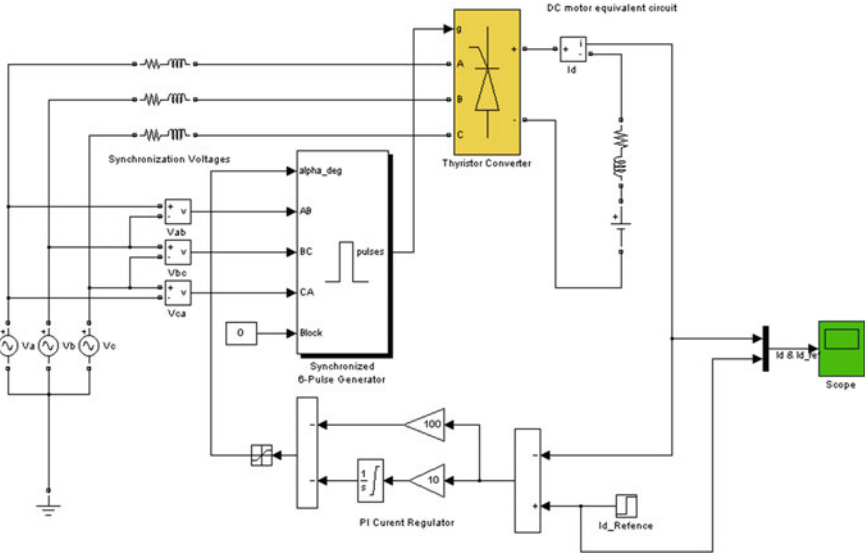


Fig. 3.2 Three-phase thyristor rectifier in closed loop

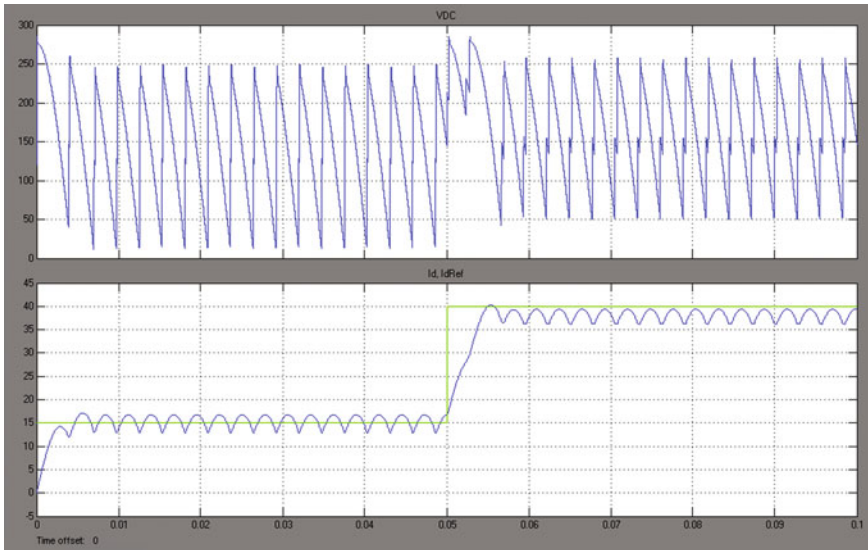


Fig. 3.3 VDC and LDC waveform for $P-I$ gains ($P = 100, I = 0$)

voltage (configuration detailed in Fig. 2.2). The output of this block is DC voltage that is connected across a motor load, denoted by a DC source, a resistor, and an inductor in series.

In accordance with the description of closed-loop system, the ‘plant’ here is the thyristor converter. This plant is represented as a Simulink[®] block, which abstracts the mathematical model of the block. The feedback and control blocks are represented as Laplace transform blocks.

The control parameter here is the output DC current. The block of Id_Reference is the reference current that the converter should source to the $R-L-E$ DC motor load shown. This reference current is changed from initial value of 15 A to 40 A after 50 ms.

The dynamic and steady-state response of the system is governed by the controller parameters, that is, the gains of the P , I , and D controllers. The detailed study of the effect of P , I , and D gains is carried out in the following chapters.

To get a glimpse of the effect of the P and I gains on the overall behavior of the system, let us reduce the Integrator gain to 0, so that the controller is Proportional-only controller.

Figure 3.3 shows the DC current of the converter against the reference. As seen in the response, at 5 ms, the reference (Green waveform) changes from 15 to 40 A and the DC current (Blue waveform) also changes. But the steady-state value of the current is 37 A (approximate average), just below 40 A. The difference between the steady-state value of the current and the desired reference current is called ‘Steady State Error’.

Now let us add the ‘integrator’ effect. The ‘ I ’ gain is now set to 50 and the ‘ P ’ gain is unchanged.

Figure 3.4 shows the DC current of the converter against the reference. As seen in the response, at 5 ms, the reference changes from 15 to 40 A and the DC current

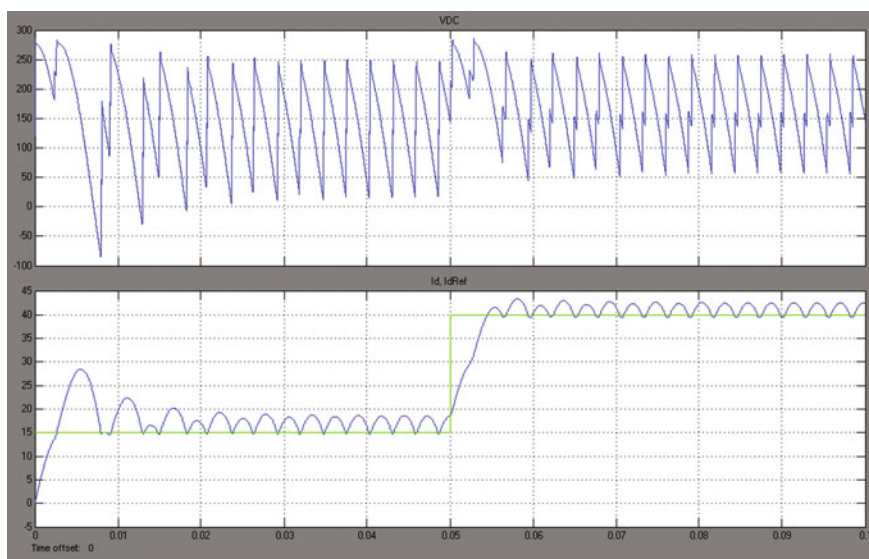


Fig. 3.4 VDC and LDC waveform for P - I gains ($P = 100$, $I = 50$)

also changes. Now, the steady-state value of the current is just about 40 Å, close to the desired reference.

A detailed analysis of the performance of the system with a change in the P , I , and D gains of the controller is performed in the following chapters.

Chapter 4

Buck Converter in Open Loop

Abstract This chapter discusses the widely used power supply buck converter topology using BUCK converter and the device used in this configuration is the MOSFET. The equations governing the open-loop system is discussed in detail and the corresponding block diagrams, topologies, and circuit diagrams are elaborated.

Keywords BUCK · Step down · Differential · Kirchoff · Freewheel · Chopper · Mathematical · PWM

An Introduction to Open Loop

In the previous chapters, we saw the basics of diode rectifier and Thyristor rectifier. These circuits are used in industrial applications when AC power is to be converted into DC power.

Another major application of power electronics devices is as power supplies used in electronic devices and as charger for batteries used in industrial application. For such applications, DC–DC converter is used. In this converter, the input is DC voltage and the output is also a DC voltage, transformed to a value, lower or higher than the input using switching power electronics devices like MOSFET. The power device is switched ON and OFF at a high frequency to generate the desired output voltage. One such DC–DC converter used in industrial application is the buck converter also known as step down chopper.

In this chapter, we will study the basics and the closed-loop control of the buck converter.

Figure 4.1 is the buck converter, also known as the ‘Step down chopper’. This power circuit consists of a power switch such as a MOSFET, represented as an arrow. This power switch is switched ON and OFF at a high switching frequency.

The behavior of this system changes based on the ON or OFF positions of the power switch. The behavior of the buck converter can be modeled by differential equations or the circuit when the power switch is ON or OFF.

Sample Circuit (Fig. 4.1):

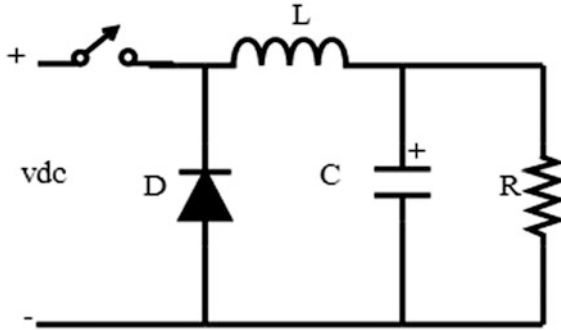


Fig. 4.1 The buck converter circuit. The *arrow* represents the power switch which is switched ON and OFF at very high frequency. The direction of the *arrow* is the direction of flow of current when the switch is turned ON

Switch ON:

Let us consider the state when the power switch is in ON condition. This connects the positive end of the power supply to the cathode of the diode. So, the diode D is reverse biased. During the ON time of the switch, the DC source causes a current *i* to flow through the inductor, capacitor, and resistor (Fig. 4.2).

Considering the output voltage of the converter across the resistor to be V_o , apply Kirchoff's voltage law to the circuit:

$$\begin{aligned}
 V_{dc} - L \frac{di}{dt} - V_o &= 0 \\
 L \frac{di}{dt} &= V_{dc} - V_o \\
 \frac{di}{dt} &= \frac{V_{dc} - V_o}{L}
 \end{aligned}
 \tag{4.1}$$

Fig. 4.2 The buck converter circuit when the switch is switched ON

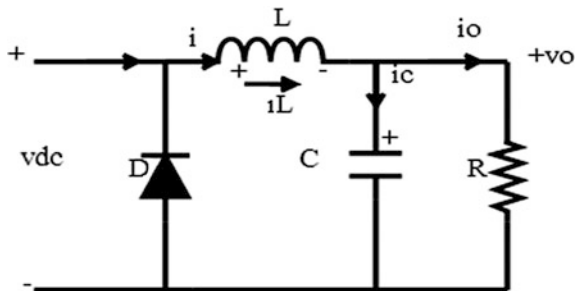
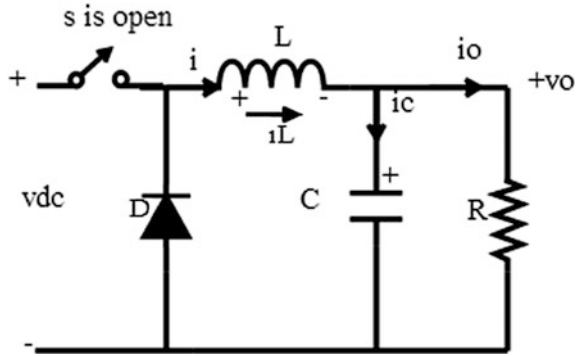


Fig. 4.3 The buck converter circuit when the switch is switched OFF



Switch OFF:

Now let us consider the state when the power switch is in OFF condition. When the switch is turned OFF, the inductor does not allow a sudden change in current. So, effectively, the polarity of the charge on the inductor is reversed to oppose this change in current. This causes a negative potential to develop at the cathode end of the diode. This forward biases the diode. This causes the current to *freewheel* through the diode, inductor, and the load resistor (Fig. 4.3).

Applying Kirchoff’s voltage law, the differential equation that governs the system in the OFF time of the switch is thus:

$$L \frac{di}{dt} - V_o = 0 \quad \frac{di}{dt} = \frac{V_o}{L} \tag{4.2}$$

From (4.1) the change in inductor current during the ON time of the switch.

$$\Delta I_{ON} = \frac{-V_o + V_{dc}}{L} * T_{ON} \tag{4.3}$$

From (4.2) the net change in the inductor current during the OFF time of the switch is

$$\Delta I_{OFF} = \frac{V_o}{L} * T_{OFF} \tag{4.4}$$

According to the inherent property of the inductor, the net current in the inductor during the complete cycle should be zero. Thus,

$$\Delta I_{ON} = \Delta I_{OFF} \tag{4.5}$$

From (4.3) and (4.4):

$$\begin{aligned}
 \frac{-V_o + V_{dc}}{L} * T_{ON} &= \frac{V_o}{L} * T_{OFF} \\
 (-V_o + V_{dc}) * T_{ON} &= V_o * T_{OFF} \\
 \therefore V_o(T_{ON} + T_{OFF}) &= V_{dc} * T_{ON} \\
 \frac{V_o}{V_{dc}} &= \frac{T_{ON}}{T_{ON} + T_{OFF}}
 \end{aligned} \tag{4.6}$$

The duty cycle of the power switch is defined as the effective ON time of the switch. So the duty cycle of switch is defined as:

$$D = \frac{T_{ON}}{T_{ON} + T_{OFF}} \tag{4.7}$$

From (4.6) and (4.7), for the buck converter (step down chopper):

$$\frac{V_o}{V_{dc}} = D \quad \text{or} \quad V_o = D * V_{dc} \tag{4.8}$$

From the equations, it is obvious that duty cycle (D) is always less than 1 and the maximum value is 1 (Switch is ON for 100 % of the time).

Thus from (4.8) it is clear that

$$V_o < V_{dc} \tag{4.9}$$

Thus, the circuit of the Buck converter produces an average output voltage that is less than the input voltage.

Mathematical Modeling of the Power Converter

Equations (4.1) and (4.2) are the very basic power equations that give the information about the buck converter.

Combining Eqs. (4.1) and (4.2), the generic equation for the rate of change of induction current is:

$$\frac{di}{dt} = \frac{x * V_{in} - V_o}{L} \tag{4.10}$$

where $x = 1$ when switch is ON and $x = 0$ when switch is OFF.

The current in the circuit can be integrated over the duty cycle as:

$$i = \int \frac{di}{dt} dt \quad (4.11)$$

Current capacitor C is given by *

$$i = C * \frac{dV_o}{dt}. \quad (4.12)$$

Thus

$$V_o = \frac{1}{C} * \int i_c dt \quad (4.13)$$

Applying Kirchoff's current law:

$$i_c = i_L - i_o \quad (4.14)$$

where i_L is the current inductor, i_o = output current in load, and i_c is the capacitor current.

Also,

$$i_o = \frac{V_o}{R}. \quad (4.15)$$

Thus,

$$i_c = i_L - \frac{V_o}{R} \quad (4.16)$$

Equations (4.7), (4.9), (4.10), and (4.11) can be combined together to develop the mathematical model the buck converter (Fig. 4.4):

Setting V_{in} to 100 V and duty cycle at 80 %, the output should be $V_o = D * V_{in} = 0.8 * 100 = 80$ V.

The Control of the Buck Converter

The buck converter is used in different applications that involve conversion of a higher voltage to a lower voltage DC, such as small SMPS power supplies, inverter batteries, etc.

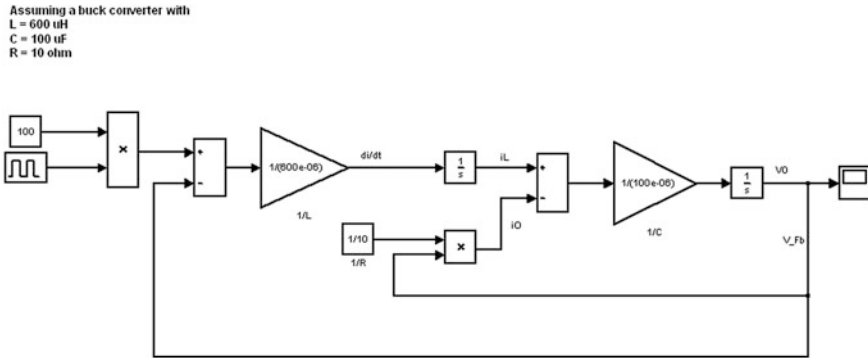


Fig. 4.4 Mathematical model of the open-loop buck converter

Assuming that such buck converter is used for charging a battery in UPS, the input to the buck converter will be a DC voltage, coming from an uncontrolled full bridge diode rectifier. The input to the diode rectifier will be from a utility power station.

Since the supply from utility power is not a steady supply, there will be variations in the input AC for the rectifier. This would change the DC input to the buck converter. Thus, according to Eq. (4.6), the output voltage of the converter will change according to the configured duty cycle. This would change the charging voltage of the battery and may damage the battery, even resulting in an explosion.

Thus, it is required to maintain the output voltage of the buck converter constant, even if the input voltage from the utility power changes.

One way to maintain the charging voltage to the battery constant is to connect a variable tap transformer at the input of the diode bridge and monitor the voltage from utility. If there is a rise in the utility voltage, the transformer turn ratio is *manually* reduced to maintain the input voltage to the bridge rectifier the same as before the increase in utility voltage. Similarly, the turn ratio is increased if there is a fall in the utility voltage. Such a manual control is called *Open-Loop Control*. An open-loop control system does not involve any *automatic feedback* mechanism.

Another mechanism that maintains the output voltage of the buck converter constant for any changes in the input involves a self-adjusting system, where the *controlled parameter* is changed automatically for changes in the input, using a *feedback* mechanism. Such control is called *Closed-Loop Control* and is the most widely used control mechanism in all practical systems.

Voltage Mode Control of Buck Converter

In the DC–DC buck converter a DC voltage at one level is converted into a DC voltage at another level by *switching* a power switch like a MOSFET. Such switching mechanism is called *Pulse Width Modulation (PWM)*. In such system, the *frequency* of the switching is constant, but *duty cycle* is variable.

Consider the buck converter circuit modeled above with the parameters L , C , and R set to the values shown in the figure. This is an open-loop model of the converter. It can be seen from Eq. (4.6) that the output voltage is proportional to the input and the proportionality factor is the duty cycle D .

Thus, due to change in the utility supply, if the DC voltage input V_{in} to the converter changes from 100 to 150 V, the output can be maintained constant to 80 V if the duty cycle is changed from 80 % to 53.33 %.

Also, due to change in the utility supply, if the DC voltage input V_{in} to the converter changes from 100 to 90 V, the output can be maintained constant to 80 V if the duty cycle is changed from 80 to 88.88 %.

So now we have a parameter in duty cycle that can be changed to maintain the output voltage of the buck converter constant for changes in the input voltage. This parameter is called *control parameter*.

The desired voltage at output of the converter is 80 V. The *desired* value is known as the *reference*. Under ideal conditions, when the output is equal to the reference, the system is said to be in a *steady-state* condition.

When the input or load on the converter undergoes a change, the output voltage tends to change and follow the change in the input. This creates a difference between the reference and the output. This difference is called the *error*.

In the next chapter, we will see how the control parameter is automatically adjusted using a *feedback* mechanism.

Chapter 5

Buck Converter in Closed Loop

Abstract This chapter discusses the closed-loop control of the open loop BUCK converter discussed in the earlier chapter. The closed-loop design is illustrated with the Simulink[®] model and the corresponding waveforms for different control parameters of proportional, integral, and differential gains.

Keywords PID · PI · PWM · UPS · Instability

An Introduction to Closed Loop

In the previous chapter, we saw the basics of the buck converter and converted the power circuit of the buck converter into mathematical equations using the differential equations governing the system.

In this chapter, we will study the closed-loop control of the buck converter (Fig. 5.1).

A scaled down output voltage is used as a Feedback. This is the closed-loop model of buck converter with the *PID* controller. The reference voltage is 80 V and input voltage is variable.

The prime purpose of the so-called '*PID controller*' is to adjust the duty cycle of the power switch such that for changes in input voltage and load, the output voltage is *controlled* to 80 V.

A study of the effect of the gains of the *P*, *I*, and *D* controllers on the overall dynamics of the closed-loop system is described below.

In order to maintain the output voltage constant, the controller should adjust the duty cycle of the power switch when the input voltage or the load changes. This is achieved by the *PI* controller. A usual challenge in control engineering is to decide upon the *starting* gains for the *P* and *I* controller, which can be changed later to fine-tune the system performance.

The difference between the reference (80 V) and the *feedback* is called 'Error'. For the DC–DC converter, this error is a DC value. To *generate* a PWM pulse for

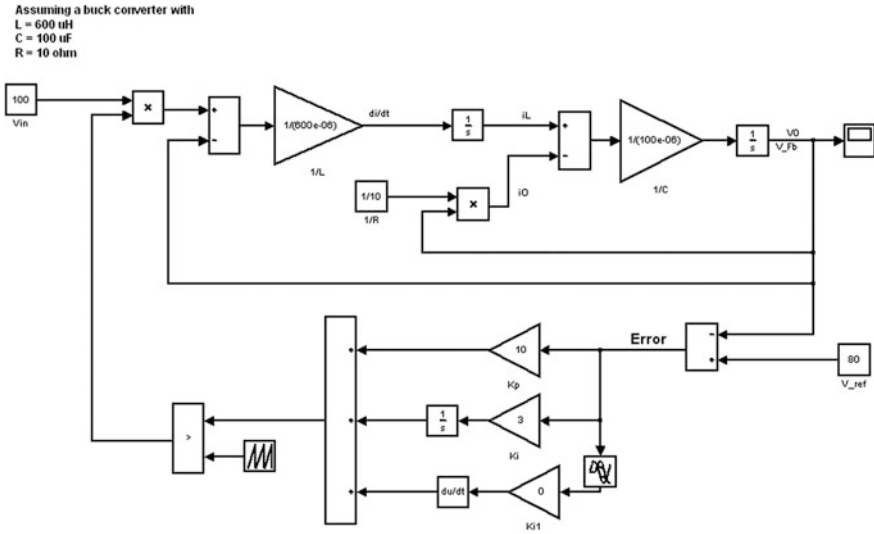


Fig. 5.1 The buck converter in voltage mode control

the power switch, this error is compared with a saw-tooth voltage pulse, as indicated by the ‘Repeating Sequence’ block in Fig. 5.1, using an electronic *comparator* action. In an analog PWM controller chip, such saw-tooth voltage is generated at fixed amplitude. For demonstration purpose, the peak of this voltage in the simulation is assumed to be 50.

Since the comparator will give a zero output for any amplified error value above 50, the gains of the *PID* controller should be such that the amplified error is below 50. This is the starting point to decide the controller gains.

Let us start with a very small proportional (*P*) gain of 0.05 and the *I* and *D* gains as zero (Fig. 5.2).

Experimentally, it is seen that for this gain value, the ‘error’ is 72 V, and the output voltage is nearly 8 V DC, which is far off from the reference of 80 V. This is expected, because the amplified error after multiplication by the *P* gain of 0.05 is 3.63 and when compared with a saw-tooth voltage of 50 would result in very less ON time for the switch and thus, very low duty cycle. Thus, intuitively, it can be seen that if the *P* gain is increased, the ON time of the switch would increase, resulting in an output that is close to the reference of 80 V.

Now, if the *P* gain is set to a sufficiently high value, say 100, it is expected that we would reach the reference of 80 V without any further adjustments in the gains.

Figure 5.3 shows the output voltage of the system with a *P* gain of 100 and the *I* and *D* unchanged at 0.

From Fig. 5.3, it is seen that the output is close to the reference of 80 V, but there is a large *ripple* in the voltage of close to 6 V. Such ripple is an undesired effect of the control system. This phenomenon is seen because a very large *P* gain causes the DC input of the comparator to momentarily shoot above 50 and then returns below

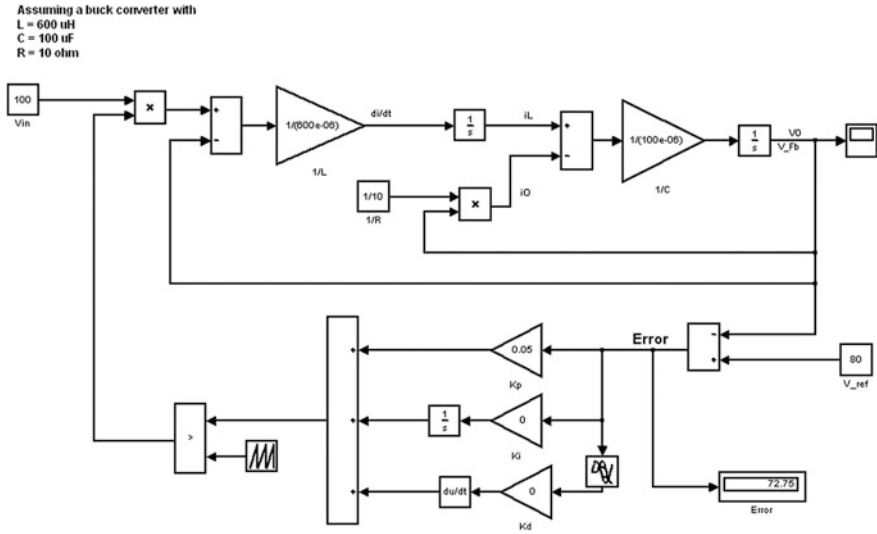


Fig. 5.2 The buck converter in voltage mode control. For $P = 0.05$, $I = 0$, $D = 0$, the ‘Error’ between the reference (80 V) and actual voltage is ~ 72 V, thus the output voltage is 8 V, far off from the desired 80 V reference

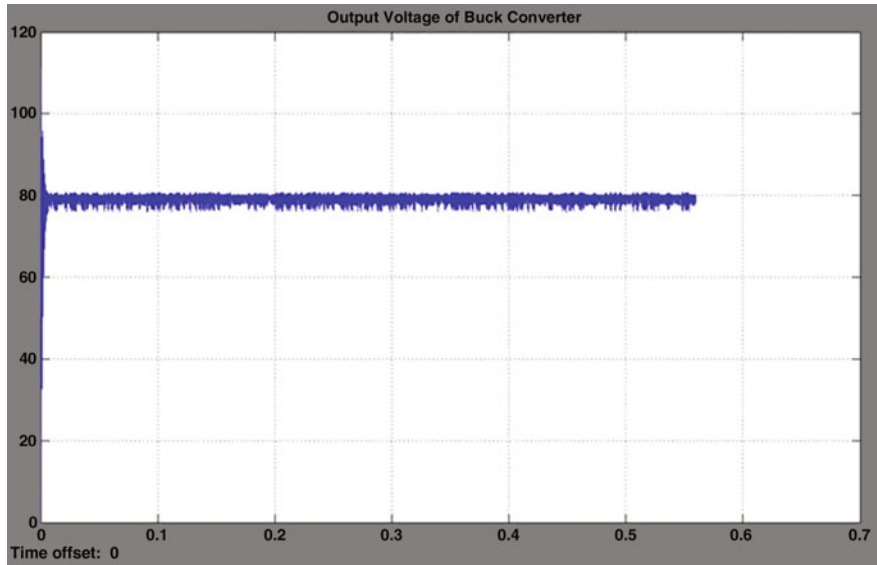


Fig. 5.3 Output DC voltage of the buck converter. A large ripple is seen in the output voltage for a significantly large P gain of $K_p = 100$, $K_i = 0$, $K_d = 0$

50 to a very low value due to the closed-loop control action. So, there is a continuous change from very less to very high duty cycle, thus causing a ripple in the output voltage.

From this experimentation it can be seen that a very low P gain, below 10 causes a very large error and deviation from the reference voltage and a large P gain of above 50 causes a large ripple in the output voltage. Thus, a starting gain of 10 for the P controller is a reasonable starting point for the control system (Fig. 5.4).

Let us assume that the closed-loop system consists only of a proportional ‘ P ’ controller. This means that the gains for the ‘ I ’ and ‘ D ’ controller are zero as shown in the above figure. Let us study the response of the controller with only ‘ P ’ controller.

Figure 5.5 shows the Simulink® oscilloscope for output voltage of the buck converter with only the proportional controller. As seen in this figure, for reference voltage of 80 V, the output voltage with the ‘ P ’ controller stabilizes at about 76 V. This difference of 4 volts from the reference is a typical behavior of the ‘ P ’ controller. This difference is called the ‘*Steady-State Error*’ of the system.

The steady-state error is a phenomenon that may be acceptable for some systems but may not be acceptable for other systems. For example, in an application like a UPS battery charger, a difference of a few volts from the desired reference may cause the system to draw excess current causing overheating of the battery.

In systems where the steady-state error is not acceptable, this ‘error’ between actual output and reference can be eliminated completely by *integrating* the difference between reference and feedback over a period of time. This integration effect in the closed-loop parlance is called the ‘*PI controller*’. The effect of the PI controller is described below.

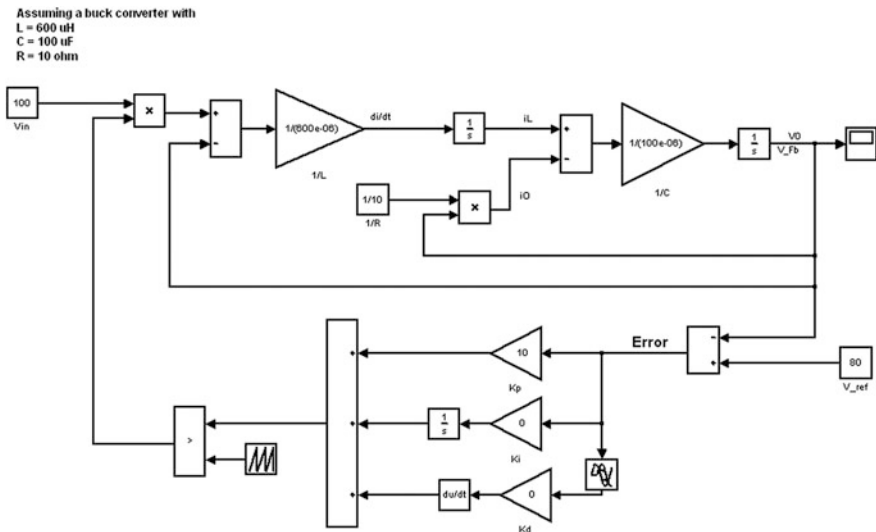


Fig. 5.4 The buck converter in voltage mode control for $K_p = 10$, $K_i = 0$, $K_d = 0$

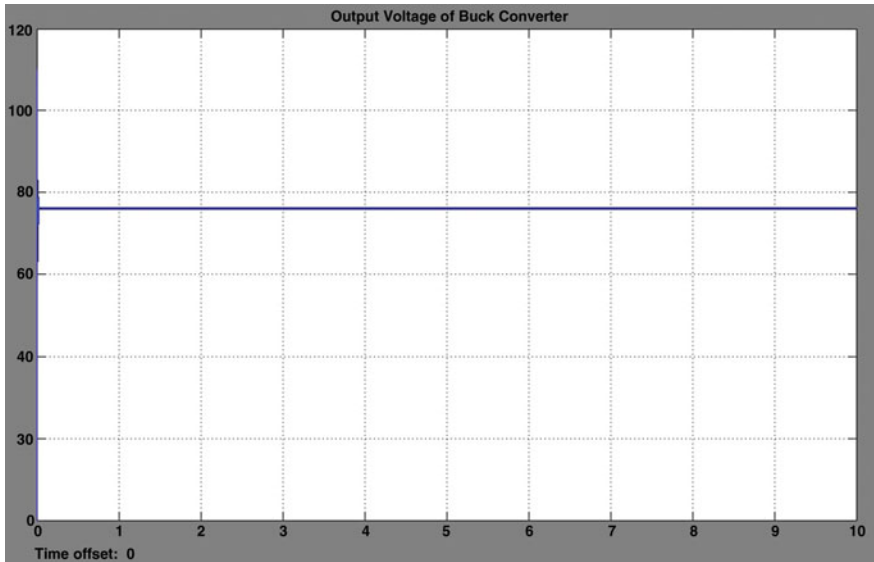


Fig. 5.5 Simulink oscilloscope for output voltage. For $K_p = 100$, $K_i = 0$, $K_d = 0$, there is a steady-state error of 4 V in the output voltage of the converter

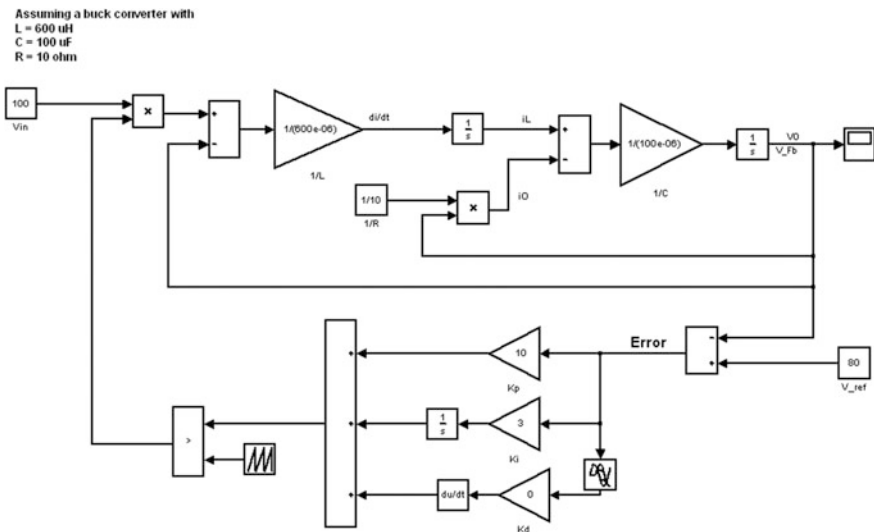


Fig. 5.6 The buck converter in voltage mode control for $K_p = 10$, $K_i = 3$, $K_d = 0$

Figure 5.6 shows the PI controller where the proportional gain is 10 and integral gain is 3. The reference is set to 80 V and input is variable.

The response of the PI controller on the output voltage is shown in Fig. 5.7.

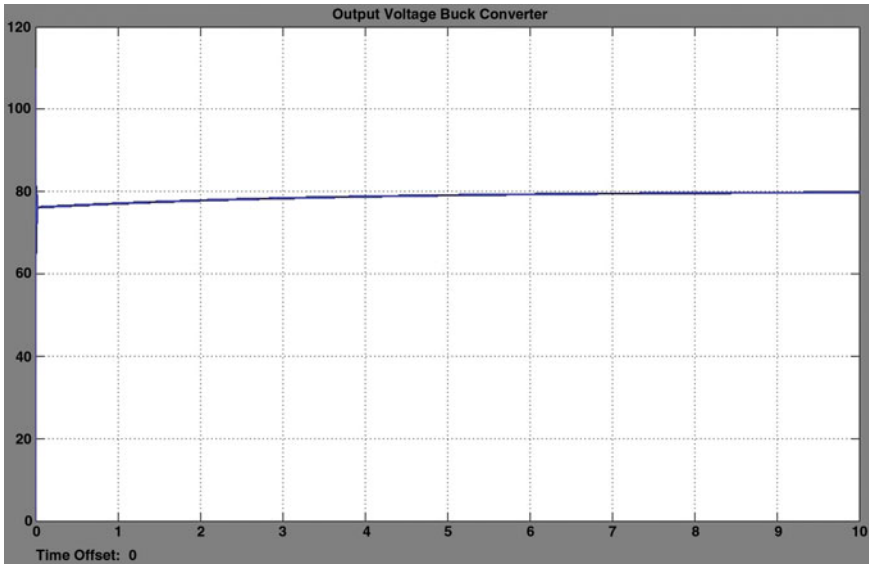


Fig. 5.7 Simulink[®] oscilloscope for output voltage. For $K_p = 100$, $K_i = 3$, $K_d = 0$, the steady-state error in the output voltage progressively decreases and becomes zero after ~ 9 s

As seen in the Simulink[®] oscilloscope, the output voltage of the converter after about 10 s reaches 80 V. Effectively, the ‘error’ between reference and feedback output voltage is integrated to zero and the output voltage reaches the reference voltage of 80 V. Thus, in effect, the *PI* controller in the closed loop will reduce the steady-state error to zero.

Another obvious effect of the *PI* controller is that the response of the system is slower than that with only *P* controller. Thus, whereas the output voltage reaches the *final* value of 76 V in less than 200 ms with *P* controller, it takes about 9 s for the voltage to reach the *final* value of 80 V with the *PI* controller.

Let us take a closer look at the transient behavior of the *PI* controller (Fig. 5.8).

As seen in the above plot of the output voltage, just when the buck converter is started, the voltage goes through an overshoot and undershoots from the reference. Shown below is the zoomed voltage waveform in the initial 30 ms.

From Fig. 5.9 it can be seen that the initial overshoot is 110 V and takes about 20 ms before the voltage reaches the *final* value of 76 V. This time is called the *Settling Time*. In some applications, the settling time of 20 ms is too much.

In order to reduce the settling time, the error (difference between reference and feedback voltage) is *differentiated* over a period of time. This effect is called the *differential controller* or the *D controller*. This differentiation action has the effect of reducing the settling time, thus making the dynamic response of the system faster. Let us introduce a very small ‘*D* controller’ in our buck converter controller and see the effect.

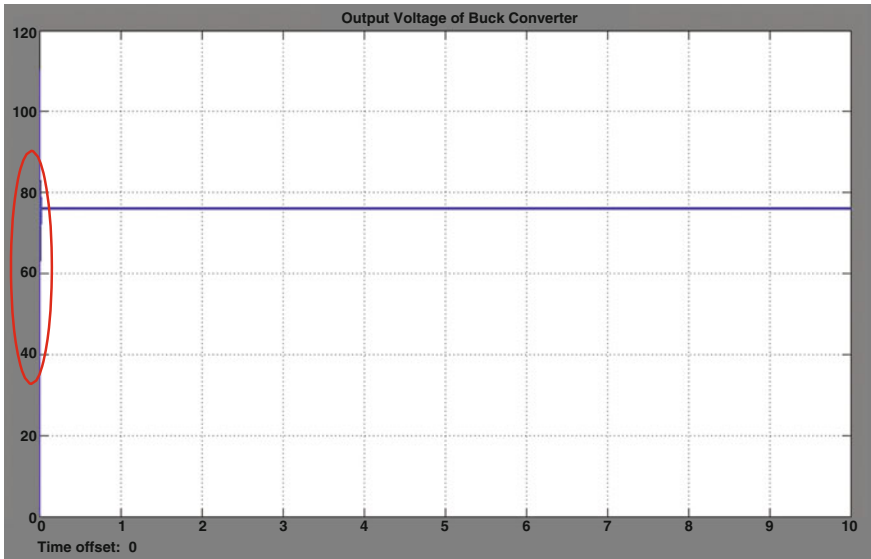


Fig. 5.8 Output voltage of the converter. Plot of the output voltage of the converter in the conditions, same as in Fig. 5.4. The transience in the system is more pronounced at start-up, as shown in the *marked section* in the plot

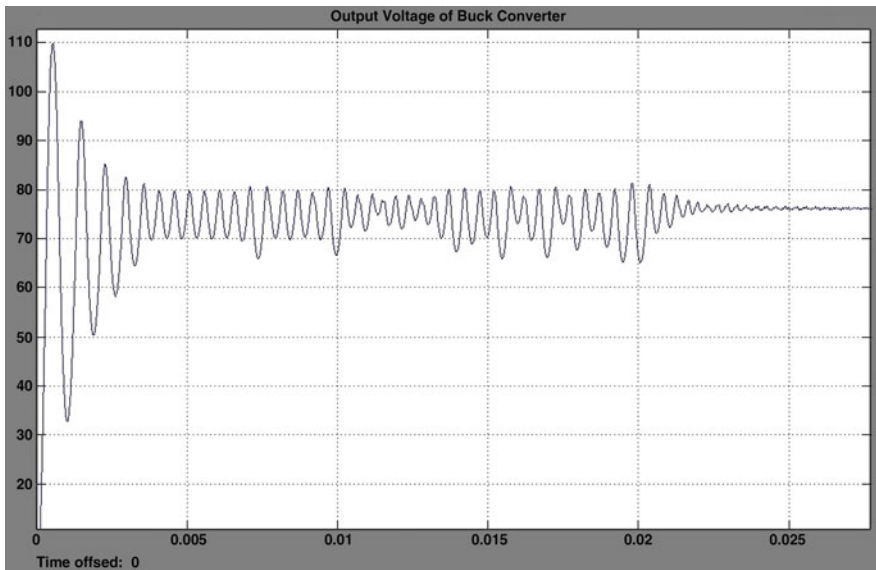


Fig. 5.9 Plot of the output voltage of the converter with the initial 25 ms zoomed

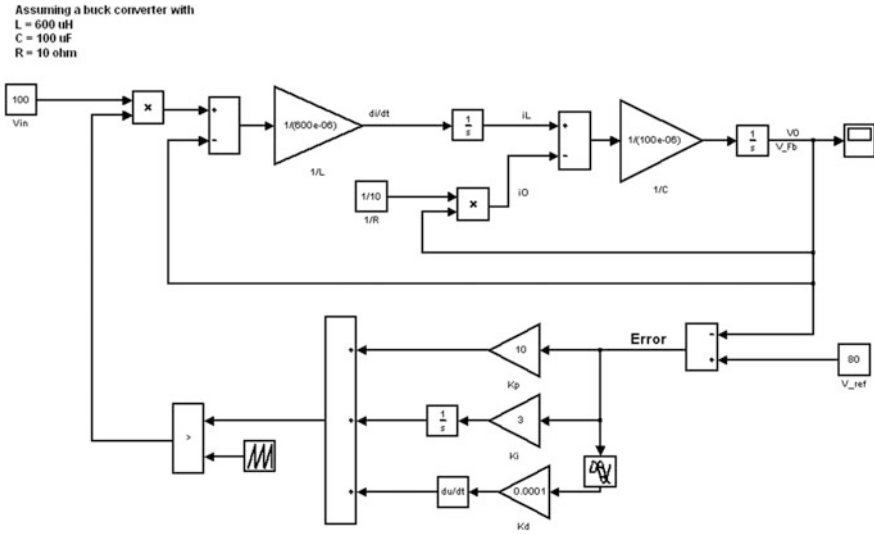


Fig. 5.10 The buck converter in voltage mode control for $K_p = 10$, $K_i = 3$, $K_d = 0.0001$

Figure 5.10 shows the closed-loop buck converter with the P gain of 10, I gain of 3 and a D gain of 0.0001, thus in effect forming the so-called ‘ PID controller’.

Figure 5.11 shows the output voltage waveform with the PID controller. Let us zoom again in the initial 30 ms region.

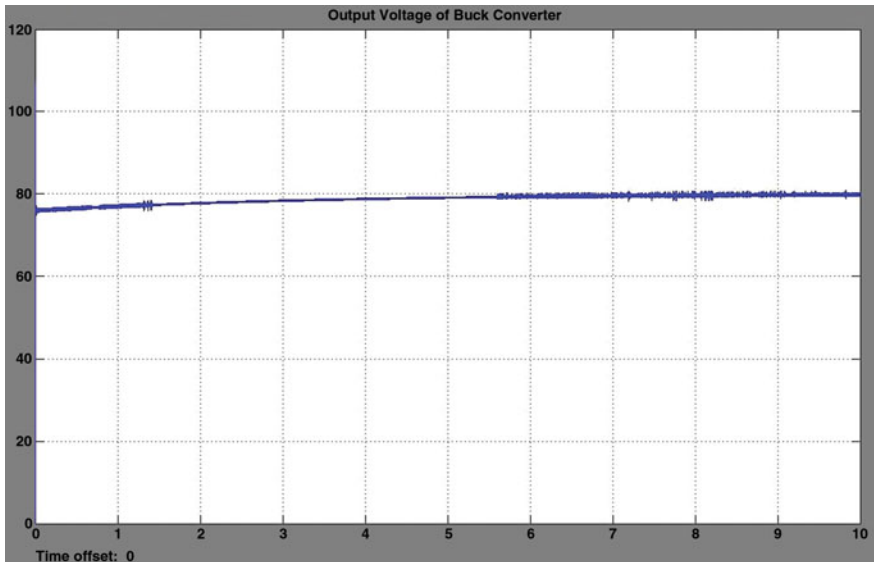


Fig. 5.11 Plot of the output voltage of the converter with $K_p = 10$, $K_i = 3$, $K_d = 0.0001$. Due to the integrating effect of the I controller, the steady-state error progressively decreases and also the initial transient response is improved, as shown in the next plot.

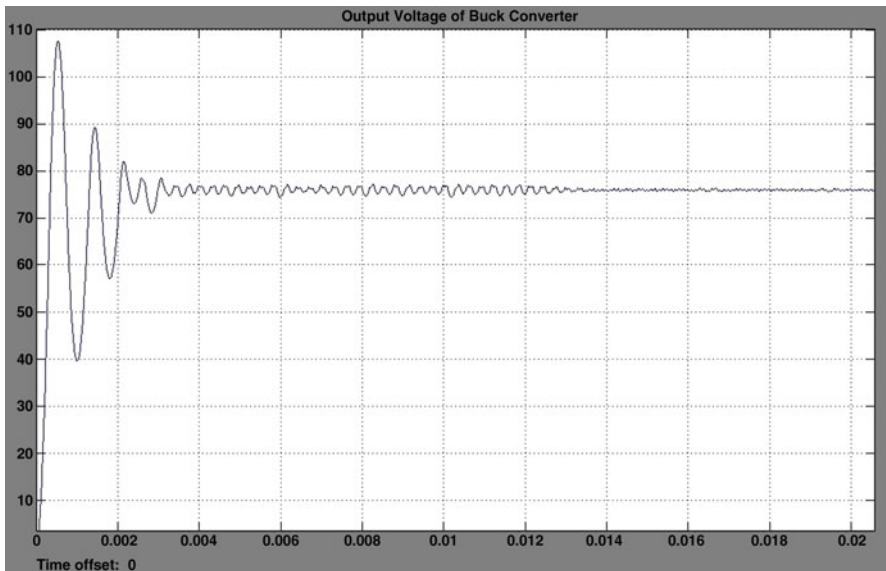


Fig. 5.12 Plot of the output voltage of the converter initial 20 ms zoomed. It is evident that the voltage stabilizes faster, in about 14 ms, compared to ~25 ms as shown in Fig. 5.8, without the *D* controller

From Fig. 5.12 it can be seen that the initial overshoot is 105 V and it takes about 12 ms before initial transience is reduced and voltage starts reaching toward the final value of 80 V. Thus, by introducing the differentiation action in the loop, the initial dynamic response is improved and settling time is reduced from 20 to 12 ms.

However, the ‘*D*’ controller may further introduce instability in the system depending on the plant to be controlled. For this reason, generally, the differential controller is not required and a ‘*PI* control’ should be enough to stabilize the system.

Thus, it can be seen that a stable control system that meets the specified design criterion can be designed by properly adjusting the *P*, *I* and *D* gains of the controller.

Chapter 6

Design of Embedded Control

Abstract This chapter discusses the implementation of the analog controller discussed in the earlier chapter as a digital controller. The conversion is mathematically represented and translated into implementable code for microprocessors.

Keywords Analog · Digital · Discrete · Intelligence · Embedded · Sampling · z-transform

Introduction

In Chap. 5, we saw a simple controller with P , I , and D controllers in which the gains of the P , I , and D controllers are designed so as to achieve the specified design criterion for the system. This example is derived from applications based on the MATLAB[®] and Simulink[®] technical computing environment-based modeling. In this chapter, we will see how such controller is designed in a physical system. The control action, as mentioned in the previous chapter can be achieved by either an *Analog* or a *Digital* controller.

With the evolution of integrated circuits (ICs), the initial control systems were developed using Analog controllers. An analog controller typically is an IC that implements the P , I , and D control action along with analog interface devices that are linear amplifiers.

Analog and Digital Control

Figure 6.1 shows the block diagram representation of the buck converter explained in Chap. 5 when the controller is Analog. The analog controller shown here is a part of an IC. The controlled variable (output voltage) is connected to a sensor that scales down the high voltage from the plant with IC-specific low voltage. The

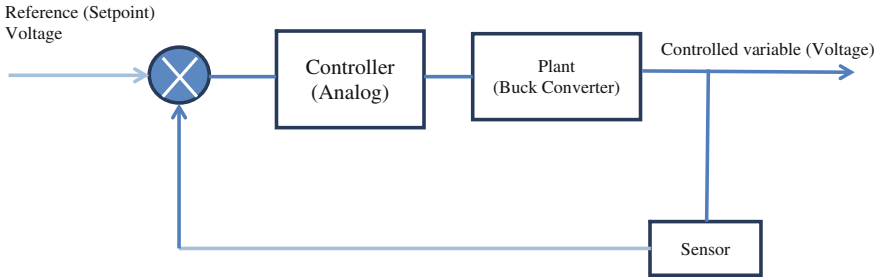


Fig. 6.1 Buck converter block diagram with analog controller

output voltage is generated according to Equation $V_o = D * V_{in}$, where D is the duty cycle that is changed by the controller to get the output close to the reference voltage.

In the Analog controller shown here, any change in the output will be sensed by the sensor and connected to the feedback *instantaneously*, thus adjusting the duty cycle. Thus, intuitively, the Analog controller is fast and good enough to meet our design criterion. However, the analog controller like the one shown here suffers from certain drawbacks.

Consider for example if you have to change the P , I , or D controller gains for tuning the controller. For changing the gains, some resistor in the analog circuit needs to be de-soldered and replaced with a new resistor to get a proper gain. This involves significant skills, time, and resources. Also, since resistors are available only for certain values, an exact gain will be difficult to achieve.

Consider another case when the controller, instead of a simple PID controller is a complicated third-order transfer function. To implement such complex transfer function, a large circuit consisting of combinations of ICs, operational amplifiers, and many discrete electronics components will be required. This will require a significant space on the circuit board and will add to the cost of the system.

The drawbacks mentioned above can be overcome using a *digital* controller instead of the traditional analog controller.

With the progress and advancement in computer technology, it has become possible to build in *intelligence* in an industrial system using microcontrollers and high speed Digital Signal Processors (DSPs). An electronic circuit with a built-in intelligence using a microcontroller or DSP along with analog and digital interface circuits and an on-chip system-specific embedded software (firmware) is called as an 'Embedded System'.

Figure 6.2 shows the block diagram representation of the Buck converter with a *Digital* controller instead of the Analog controller. The *Digital* controller implies that the controller is developed as *embedded software* instead of the traditional method of discrete electronic circuit components.

The embedded software is developed in a microcontroller. Since the microcontroller, which is a small computer, will need all the information in the computer

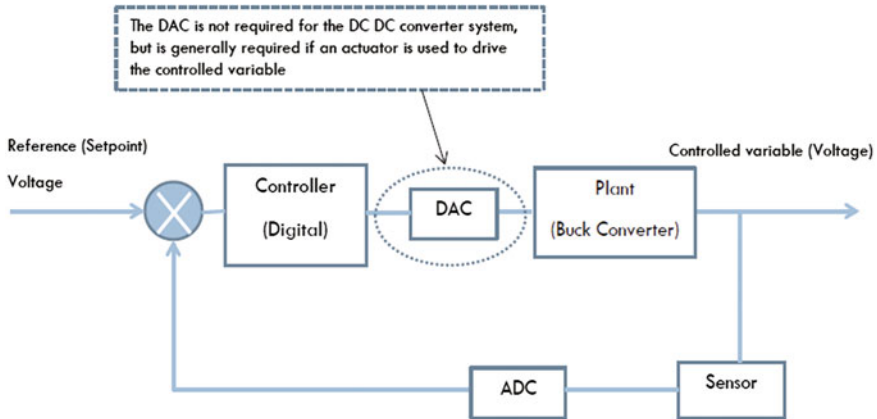


Fig. 6.2 Buck converter block diagram with digital controller

specific (digital) format, the output from the sensor is converted from analog (continuous) into digital (sampled). This transformation of data is performed by the semiconductor device called *Analog to Digital Converter*. In the process of A to D conversion, the values of the continuous signal are measured at discrete intervals. Each of these measurements is called as *sample* and the process is called *sampling*.

The interval between successive samples is called sampling time (T_s) and the inverse of the sampling time is called *sampling frequency*.

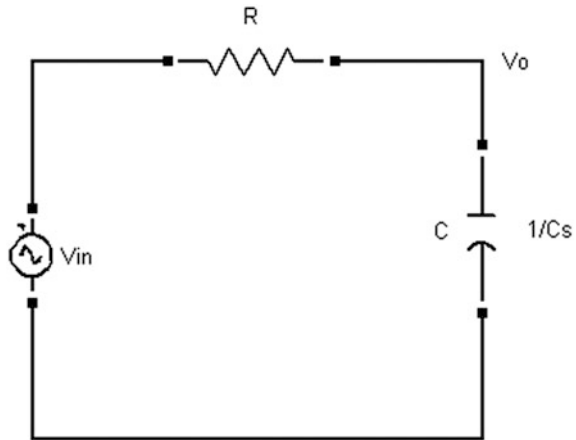
In certain industrial systems, an actuator may be required to drive the controlled output. For example, if the controlled variable is the precision position of a Robotic arm, the motor controlling the position of the arm requires voltage of a particular magnitude and for a particular time to position the robot arm. In such case, the digital output of the controller needs to be converted into continuous (Analog) voltage. This is performed by the semiconductor device called *Digital to Analog Converter*.

Developing an Embedded Controller

In Chap. 5 we saw the modeling of the DC–DC buck converter using differential equations and converting these equations into Simulink[®] block-based model. Laplace transform is the best and the most popular method of such type of analog modeling. Electronic circuits that implement the *PID* controller can be mathematically modeled using Laplace transform. Now, we will see the basics of designing a digital controller that is converting the controller logic into a piece of *embedded software*.

The Laplace transform forms the basis of modeling any physical system. However, this transform is fundamentally based on the assumption that the system to be modeled is *continuous* (analog). To design a digital controller, the system equations

Fig. 6.3 First-order low pass filter



based on Laplace transform need to be further transformed into a discrete (digital) domain. Such transform that helps to convert the Laplace transform based system model equations into sample-based (digital) equations is the ***z-transform***.

Let us take the example of converting a transfer function from Laplace to z transform, such that the transfer function can be implemented as embedded software.

Figure 6.3 shows a simple first-order low pass R-C filter. In terms of Laplace transform, the transfer function of this circuit is expressed as:

$$\begin{aligned} \frac{V_o}{V_{in}} &= \frac{\frac{1}{C_s}}{R + \frac{1}{C_s}} \\ \frac{V_o}{V_{in}} &= \frac{\frac{1}{RC}}{s + \frac{1}{RC}} \end{aligned} \quad (6.1)$$

The Laplace transform is used to analyze signals in continuous time systems. The discrete-time equivalent of the Laplace transform is the z -transform. The Laplace transform plane or the so called s -plane is related to the so called z -plane by the equation:

$$z = e^{st} \quad (6.2)$$

Converting this exponential into Taylor's series and rearranging the equation, the relation between the ' s ' domain and ' z ' domain can be expressed in the simplest form as:

$$s = \frac{1 - z^{-1}}{T_s} \quad (6.3)$$

where T_s is the sampling time.

From Eqs. (6.1) and (6.3),

$$\frac{V_o}{V_{in}} = \frac{\frac{1}{RC}}{\frac{1-z^{-1}}{T_s} + \frac{1}{RC}}$$

Denoting the RC time constant by $T = RC$

$$\frac{V_o}{V_{in}} = \frac{\frac{1}{T}}{\frac{1-z^{-1}}{T_s} + \frac{1}{T}}$$

Solving this equation further,

$$V_o * (T + T_s - T * z^{-1}) = T_s * V_{in}$$

Rearranging further,

$$V_o = \frac{T}{T_s + T} V_o z^{-1} + \frac{T_s}{T_s + T} V_{in} \quad (6.4)$$

The z -transform is the discrete-time equivalent of the Laplace transform. From Eq. (6.2), the ‘ z ’ operator represents a single sample. Thus, the present sample of the signal, multiplied with z , represents the next sample and the present sample multiplied with z^{-1} represents the previous sample of the signal. Thus, if the n th sample (present sample) of the input and output voltage of the RC first-order circuit are denoted by $V_{in}(n)$ and $V_o(n)$, respectively, and the previous samples of the signals are denoted by $V_{in}(n-1)$ and $V_o(n-1)$, respectively, then in terms of the ‘ z ’ operator, $V_o(n-1) = V_o * z^{-1}$ and $V_{in}(n-1) = V_{in} * z^{-1}$.

Thus Eq. 6.4 can be represented in terms of the samples as:

$$V_o(n) = A * V_o(n-1) + B * V_{in}(n) \quad (6.5)$$

where

$$A = \frac{T}{T_s + T} \quad \text{and} \quad B = \frac{T_s}{T_s + T}$$

Equation of the form (6.5) is called a difference equation.

This difference equation is a simplified digital representation of the first order RC filter circuit. The difference equation can be used to convert this system into the *embedded software*. Consider that the sampled input voltage is available in the microcontroller in the form of a C code variable as an array $V_{in}[\text{SIZE}]$ and the sampled output is available as an array $V_o[\text{SIZE}]$. A C code that implements this first-order low pass filter will look like this:

```

For (i=0; i<SIZE; i++)
{
    Vo[i] = A * Vo[i-1] + B * Vin[i];
}

```

Thus, starting from an analog circuit shown in Eq. (6.3), we have written a C code that implements the low pass filter action.

In a practical industrial control system, a similar approach is followed to convert the transfer function of the controller available in Laplace transform equation format into z -transform, reducing the z -domain equation to difference equation and then converting the difference equation into embedded software code.

A Brief Introduction to Model-Based Design

In this chapter we saw how the development of control systems is simplified with digital control using embedded control processors. Due to the advent of embedded systems and high speed microprocessors, the development time for industrial control systems has reduced. However, development of embedded control systems requires talent with expertise not only in the engineering aspects of the controlled systems but also in electronics and embedded software development.

Industries are under pressure to reduce the development time and optimize costs while still using advanced control systems and being innovative. *Model-based design* is an approach that helps industry by facilitating the development of advanced control systems faster.

In the Model-Based Design approach, graphical tools are used for design of complex control systems. MATLAB[®] and dSpace[®] are some such software that offer model-based development tools.

The primary steps in Model-Based Development are:

1. Modeling the plant
2. Modeling and designing the controller
3. Simulating and optimizing the simulation of the combined plant and controller together
4. Prototyping and validation of the prototype systems

The model-based development approach is different from the traditional design approach. Using this approach, engineers can design advanced control systems using graphical simulation software tools. Using this approach, the engineering skills and resources can be used for design and optimization of advanced control systems, prototyping and verification. The embedded software for the controller is automatically generated by the model-based design tools, thus facilitating rapid prototyping. More information about Model-Based Design can be found in the referenced literature at the end of this book.

Chapter 7

Case Study of an Embedded Control System Design

Abstract This chapter has a case study of control systems for power electronics for a DC motor. The application is developed with a power device, a speed measurement sensor, isolation between control and power electronics, and the control algorithm. All the mentioned subsystems are applied in the system design and the schematic of the system is depicted.

Keywords Hall effect · Opto coupler · Schematic · Layout · ATtiny2313

Introduction

The electric drive systems used in many industrial applications require higher performance, reliability, and variable speed for ease of controllability. The speed control of DC motor is crucial in applications where precision and protection are of importance. The purpose of a motor speed controller is to take a signal representing the required speed and to drive a motor at that speed. Microcontrollers can provide easy control of a DC motor. Microcontroller-based speed control systems consist of electronic component, microcontroller, and the LCD. In this study, implementation of speed control of DC motor fed by a DC chopper has been investigated. The chopper is driven by a high frequency PWM signal. Controlling the PWM duty cycle is equivalent to controlling the motor terminal voltage, which in turn adjusts the motor speed. In this work, development of hardware and software of the closed-loop DC motor speed control system have been explained and illustrated. The objective is to design a system with constant speed at any load condition. This means the motor will run at a fixed speed instead of varying with amount of load.

Application Overview

Brushed DC (Direct Current) motors are most commonly used in easy to drive, variable speed, and high start-up torque applications. They are available in a wide range of power from large horsepower to fractional horsepower. The speed and torque of the motor depend on the strength of the magnetic field generated by the energized windings of the motor, which depend on the current through them. Therefore adjusting the voltage to the motor (and current) will change the motor speed. In this project, speed control is based on generating and varying a PWM signal by the ATtiny2313 microcontroller.

The block diagram in Fig. 7.1 depicts all the subsystems in a motor speed control system.

The speed is generally measured using opto interrupters or Hall effect sensors. For low cost applications opto interrupters are used, but their reliability and life are low. Meanwhile Hall effect sensors are more reliable with higher life and higher cost. Hall effect sensors are transducers that measure flux and convert it into a voltage. They are placed to measure the rotor position which in turn gives the speed of the machine.

Measurement of Speed of the Motor

Hall Effect Sensor

A Hall sensor has been used to measure the speed of motor. The sensor gives a pulse every time a magnetic field passes through it. It requires signal conditioning to make the output usable for most applications which would be an amplifier and a compensation circuit.

Figure 7.2 shows a typical Hall effect sensor application circuit.

The Hall sensor has to be mounted in a way to sense the magnetic field of the rotor poles. The output of the sensor after amplification is connected to the microcontroller interrupt. Depending on the number of pulses in a given time period, the calculations are carried out to estimate the speed of the motor.

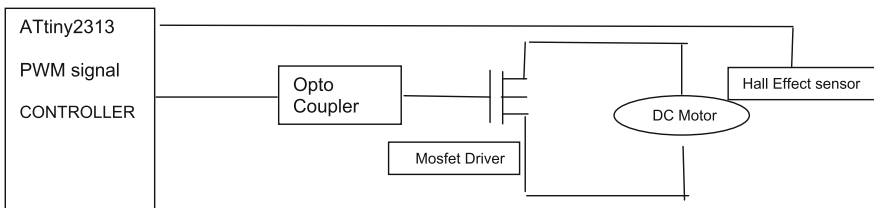
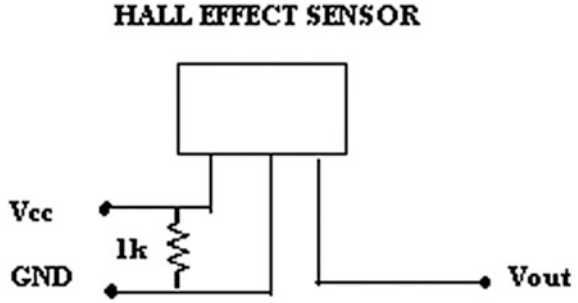


Fig. 7.1 Speed control of DC motor using PWM technique with Hall effect sensor

Fig. 7.2 Hall effect sensor



Opto Coupler

An opto coupler is a simple device which consists of a phototransistor and a LED inside the same package.

The opto coupler used in our circuit is MCT2E.

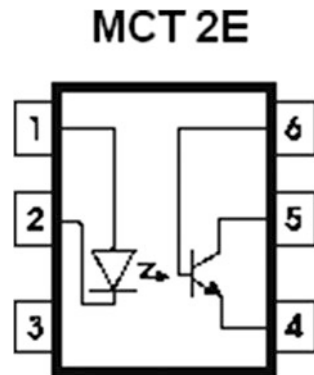
This device is extremely important in a power electronics system to isolate the control system from the power devices. The primary side of the circuit has a diode and the secondary has a transistor. The diode is a light emitting diode and the light is used as the base current for the transistor. The transistor switching on powers up the power electronics circuit and the current passes through the high current equipment. This high current equipment could be a 12 V motor or a power device like a MOSFET whose gate is connected to this transistor.

Figure 7.3 shows the opto coupler MCT2E pin out diagram.

This opto controller photodiode is switched at PWM frequency from the microcontroller and based on the duty cycle, the power output to the devices is controlled. The microcontroller output is generally at 5 V with a duty cycle from 0 to 100 %.

The isolation provided by the opto coupler keeps the ATtiny2313 chip safe from destruction.

Fig. 7.3 Opto coupler MCT2E



The opto interrupter works on the same principle of primary and secondary, the only difference being that the primary signal is kept on for the LED and the path of the light is interrupted by the interrupter simulating the magnets and hence the transistor switches ON/OFF. These signals will determine the speed of the motor.

Controlling the Speed with PWM

Adjusting the drive voltage to the motor would control the speed of the motor. The voltage applied to the armature of the motor can be changed by changing the duty cycle of the power switch (MOSFET). The higher the average duty cycle the higher the speed and vice versa.

The controlled parameter in this control system is the motor speed. The desired speed of the motor is set as the control set-point and the feedback for speed is taken from the speed sensor as described in the previous sections.

When there is an increased load on the motor, the speed of the motor will tend to fall. Based on the speed feedback from the speed sensor, the PWM duty cycle will be increased by the control system which increases the voltage to the armature, which in turn will increase the speed. Thus, the feedback control system will act in closed loop to get the motor speed to the desired set-point.

Subsystem Design

Figure 7.4 is the opto coupler internal and the PWM pulse generated by the AT-2313 microcontroller is connected to this Pin 1 of this opto coupler.

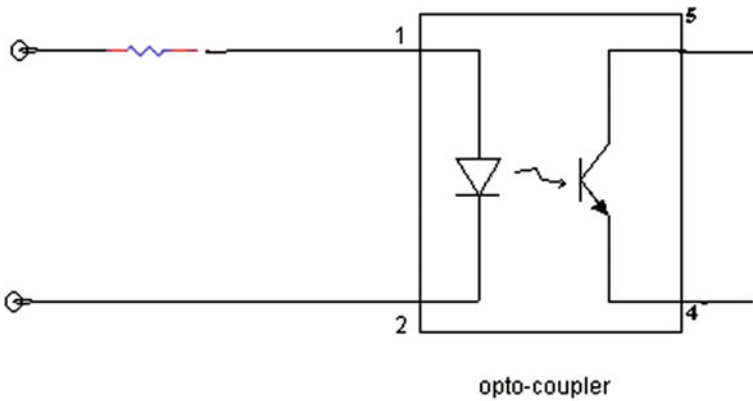


Fig. 7.4 Opto coupler details

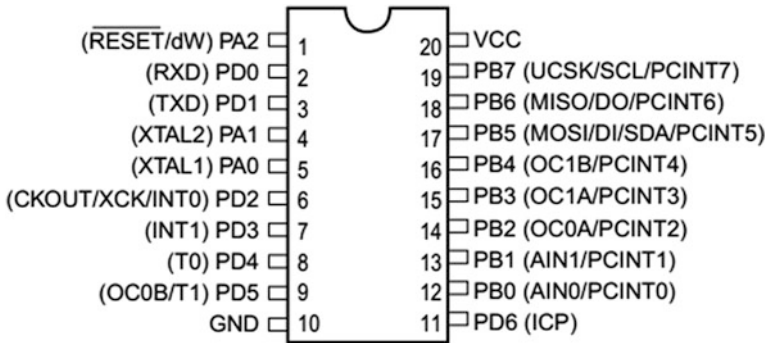


Fig. 7.5 Pin out of ATtiny2313

Figure 7.5 shows the pin out diagram of the ATtiny2313.

In this scheme, the 5 V signal from microcontroller is connected to the LED side of the opto coupler. The collector of the transistor on the Opto coupler is connected to 12 V DC. When the signal from the microcontroller goes logic High (5 V), the transistor is turned ON, which connects the 12 V DC supply to the armature of the motor and also to the base of the MOSFET. This will turn the MOSFET ON and the 12 V DC will be connected across the armature of the motor. Thus, the 5 V logic signal from the microcontroller is converted to 12 V for the motor.

The output of the Hall effect sensor is a pulse. When the magnetic north pole of the magnet comes in proximity to the Hall effect sensor the output of the Hall effect sensor becomes low. (Default output state of the Hall effect sensor is high).

The measured speed is displayed on the hyperterminal of the PC. This has been achieved by interfacing ATtiny2313 with PC using USART.

The system schematic with the MOSFET, Opto Coupler, and the Hall effect sensors is depicted in Fig. 7.6.

Two peripheral interfaces of the microcontroller are used in our scheme.

1. The external interrupt (INT1) of the microcontroller is connected to the output of the Hall effect sensor which is a pulse. On the rising edge of the signal on this pin, which is on every pulse from the Hall effect sensor, an interrupt service routine (ISR) is called. The *PI* controller is implemented in this ISR function.
2. PWM pin of the microcontroller is connected to the diode side of the opto coupler. As described in the section, the duty cycle required for the MOSFET will be calculated based on the difference between set-point speed and actual speed (in terms of counts as calculated in the ISR).

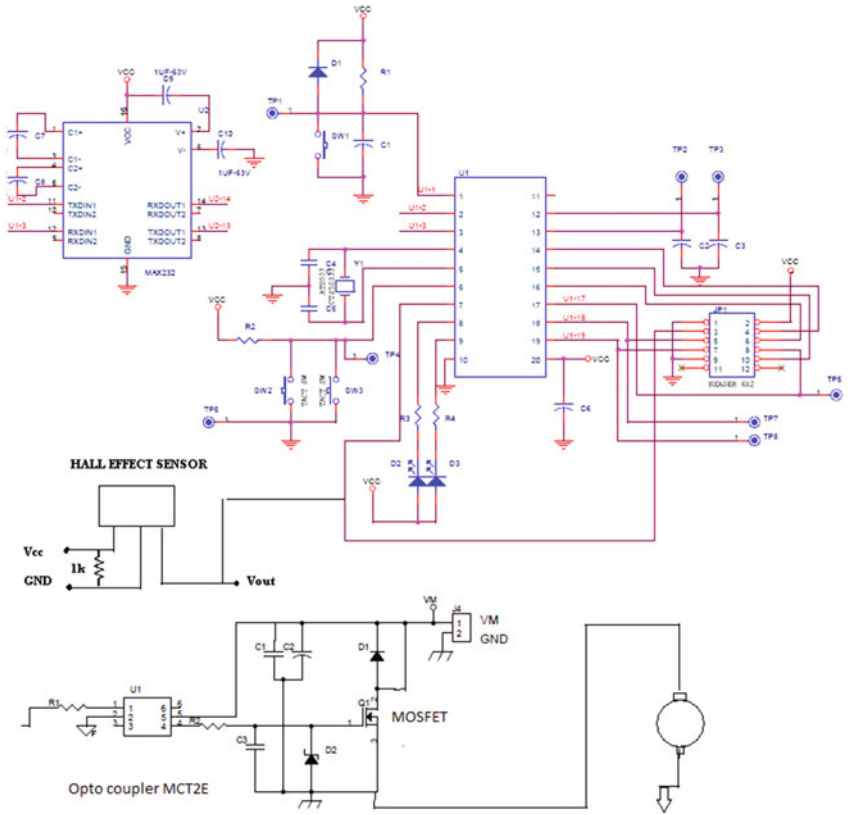


Fig. 7.6 System schematic

PCB Layout for the System

As seen in the layout diagram in Fig. 7.7, POWER connector is connected to an external DC (12 V) supply.

The connector marked USART is the Universal Synchronous and Asynchronous Receiver Transmitter. This is the serial communication feature of the microcontroller and the chip MAX232 is used for interfacing the USART from microcontroller a PC. In our scheme, the USART is used for monitoring the actual speed of the motor on a PC.

In our scheme, the sampling rate for speed is 20 μ s. In the ISR described above, the speed set-point is compared with the actual speed and the difference between the desired and actual speed is called error.

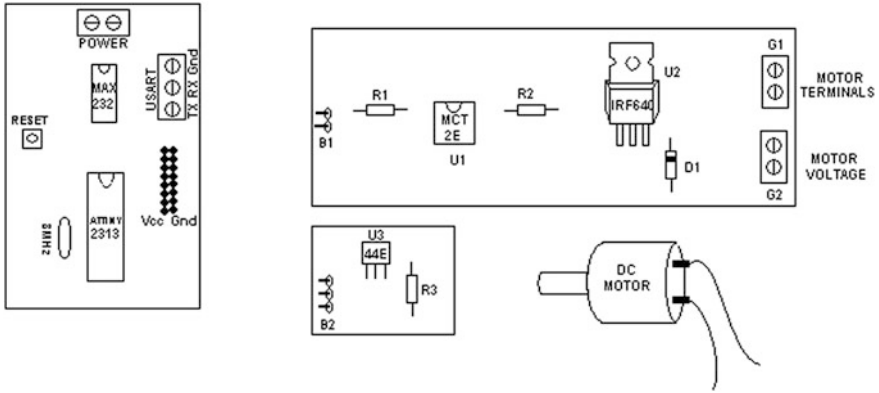


Fig. 7.7 PCB layout

The *PI* controller is implemented in the ISR. The preliminary C code for the *PI* controller is given below for reference:

```

error = setpoint_speed - measured_speed;
integral = integral + error * DeltaT;
output = kp * error + ki * integral;
    
```

where

- k_p is the proportional gain
- k_i is the integral gain
- DeltaT is the sampling time

The variable output is used for calculating the duty cycle of PWM for the MOSFET.

Conclusion

This chapter detailed the design of a closed-loop control of a DC motor using microcontroller ATtiny2313, a sensing device based on the Hall effect and the opto coupler, control of PWM duty cycle, and the power switch IRF640, thus giving the reader a complete experience on control system for power electronics application. The simulations of the control system in the earlier chapters using MATLAB[®] can be used as a starting point to develop these applications from a virtual prototyping perspective, thus enabling the engineer to reduce cost and iterations during the hardware implementation stage. The engineer can experiment different control algorithms based on the hardware platform described here.

References

1. Mohan N, Undeland T, Robbins W (2003) Power electronics converters, applications and design. ISBN 9814-12-692-6
2. Ramamoorthy M (1991) An Introduction to thyristors and their applications. ISBN 81-85336-67-9
3. All the simulation models are developed using SimPowerSystems ToolBox from Math Works®